NeuroImage 255 (2022) 119209

Contents lists available at ScienceDirect

NeuroImage

journal homepage: www.elsevier.com/locate/neuroimage

Psychological resilience and neurodegenerative risk: A connectomics-transcriptomics investigation in healthy adolescent and middle-aged females

Raluca Petrican[a,*], Alex Fornito[b], Natalie Jones[a]

[a] Cardiff University Brain Research Imaging Centre (CUBRIC), School of Psychology, Cardiff University, Maindy Road, Cardiff CF24 4HQ, United Kingdom
[b] The Turner Institute for Brain and Mental Health, School of Psychological Sciences, and Monash Biomedical Imaging, Monash University, Melbourne, VIC, Australia

ARTICLE INFO

Keywords:
Resilience
Functional brain networks
Development
Aging
Transcriptomics
Polygenic risk

ABSTRACT

Adverse life events can inflict substantial long-term damage, which, paradoxically, has been posited to stem from initially adaptative responses to the challenges encountered in one's environment. Thus, identification of the mechanisms linking resilience against recent stressors to longer-term psychological vulnerability is key to understanding optimal functioning across multiple timescales. To address this issue, our study tested the relevance of neuro-reproductive maturation and senescence, respectively, to both resilience and longer-term risk for pathologies characterised by accelerated brain aging, specifically, Alzheimer's Disease (AD). Graph theoretical and partial least squares analyses were conducted on multimodal imaging, reported biological aging and recent adverse experience data from the Lifespan Human Connectome Project (HCP). Availability of reproductive maturation/senescence measures restricted our investigation to adolescent (N = 178) and middle-aged (N = 146) females. Psychological resilience was linked to age-specific brain senescence patterns suggestive of precocious functional development of somatomotor and control-relevant networks (adolescence) and earlier aging of default mode and salience/ventral attention systems (middle adulthood). Biological aging showed complementary associations with the neural patterns relevant to resilience in adolescence (positive relationship) versus middle-age (negative relationship). Transcriptomic and expression quantitative trait locus data analyses linked the neural aging patterns correlated with psychological resilience in middle adulthood to gene expression patterns suggestive of increased AD risk. Our results imply a partially antagonistic relationship between resilience against proximal stressors and longer-term psychological adjustment in later life. They thus underscore the importance of fine-tuning extant views on successful coping by considering the multiple timescales across which age-specific processes may unfold.

Adverse life experiences can incur both immediate and long-term psychological costs by accentuating vulnerability to psychiatric and neurodegenerative disorders (Selous et al., 2020; Tani et al., 2020). Complementing a sizeable literature on the wide variety of sequelae linked to adversity, there is a rapidly expanding body of work probing the mechanisms underlying the capacity to withstand it (Gee, 2021; Murthy and Gould, 2020; Nelson and Gabard-Durnam, 2020). Psychological resilience is often conceptualised as a dynamic construct indicating positive adjustment to environmental challenges, which manifests as lower-than-expected psychopathology given experienced adversity (Collishaw et al., 2016; Feder et al., 2009; Ioannidis et al., 2020; Kalisch et al., 2017; Rutter, 2013). Whether indicative of quick recovery or active resistance to stressors, resilience is thought to stem from multilevel interactions among neural, hormonal, (*epi*)genetic, experiential, behavioral and environmental factors (Feder et al., 2009; Gee, 2021; Kalisch et al., 2019; McEwen et al., 2015).

There is compelling evidence that the mechanisms underpinning resilience change across the lifespan due to normative developmental/aging processes, as well as history of exposure and timing of stressors (Aschbacher et al., 2021; Gee, 2021; Kalisch et al., 2019; Rickard et al., 2014; Romeo, 2010; Romeo, 2018). Characterizing life-stage specific resilience processes is key to personalizing and, thus, optimizing detection and design of intervention paradigms for vulnerable individuals. To address this issue, we examined the neural underpinnings of psychological resilience against recent negative experiences (henceforth referred to as *short-term resilience*) among adolescent and middle-aged female participants in the Human Connectome Project(HCP)-Development/Aging. Short-term resilience was defined as lower-than-expected psychopathol-

* Corresponding author.
E-mail address: petricanr@cardiff.ac.uk (R. Petrican).

https://doi.org/10.1016/j.neuroimage.2022.119209.
Received 14 September 2021; Received in revised form 5 April 2022; Accepted 11 April 2022
Available online 14 April 2022.
1053-8119/© 2022 The Author(s). Published by Elsevier Inc. This is an open access article under the CC BY-NC-ND license (http://creativecommons.org/licenses/by-nc-nd/4.0/)

ogy (within the prior six months) relative to adversity experienced in the past year (i.e., number of adverse events over which the participant had little or no control, cf. Amstadter et al., 2014; Bowes et al., 2010; Collishaw et al., 2016; Rutter, 2013).

Our investigation was inspired by theories of early life adversity which posit that mechanisms underlying initial positive adjustment to environmental challenges may contribute to the long-term sequelae of stress exposure (Belsky, 2019; McLaughlin et al., 2014, 2016). We thus sought to elucidate whether the neural substrates of short-term resilience overlap those reportedly underpinning the long-term negative consequences of adversity and whether any observed relationships would vary by life stage (i.e., adolescence versus middle adulthood) (Colich et al., 2020; Ramirez et al., 2020; Rasmussen et al., 2019; Tooley et al., 2021). Our focus was on accelerated brain and biological aging, two well-documented sequelae of early life adversity predictive of later psychological vulnerability due to increased allostatic load and poorer fine tuning of the slower developing association systems transdiagnostically involved in psychopathology (Colich et al., 2020; McLaughlin et al., 2020; McTeague et al., 2017; Tooley et al., 2021). In childhood and adolescence, the two sequelae are likely interdependent, as pubertal hormones regulate brain maturation processes, while precocious functional neurodevelopment protects against accelerated cellular aging following stress exposure (Eck and Bangasser, 2020; Laube et al., 2020; Miller et al., 2020; Piekarski et al., 2017). Importantly, accelerated neurobiological aging in childhood and adolescence is regarded as an immediately adaptive response to adverse rearing environments (Belsky, 2019; Rickard et al., 2014). Specifically, precocious brain development, particularly for circuits relevant to emotion regulation, fosters successful coping, whereas earlier biological maturation (i.e., earlier pubertal timing) is posited to be evolutionarily adaptive because it maximises reproductive opportunities before an anticipated premature demise (Belsky, 2019; Brieant et al., 2021; Callaghan and Tottenham, 2016; Gee et al., 2013).

To our knowledge, a link between accelerated neurobiological aging and psychological resilience in middle adulthood has not been formally articulated. Such an association is nonetheless plausible with regards to brain aging, if quicker recovery and/or greater active resistance to stressors in later life stem(s) partly from reduced reactivity and less differentiated processing of the external environment, both of which are putative key features of neural senescence (Garrett et al., 2013, 2020; Grady and Garrett, 2018). In contrast, a positive link between resilience and accelerated biological aging, at least in the form of earlier menopausal onset, seems unlikely, given the role of ovarian hormones in dampening hypothalamic-pituitary-adrenal (HPA) axis activity following stress exposure (Engel et al., 2019; Joffe et al., 2020; Süss et al., 2021). Thus, if a relationship between biological aging and patterns of brain aging associated with resilience were to emerge, it would likely be negative.

Capitalizing on the above reviewed literature, the present study tested the model represented in Fig. 1. In short, adverse life experiences were expected to accelerate brain development/aging, both directly (Fig. 1, a-c), and via speeded biological maturation (Fig. 1, a-b-c) (Belsky, 2019; Colich et al., 2020). Our goal was to identify patterns of accelerated brain development/aging linked to resilience (Fig. 1, c-d) and probe their relevance to long-term psychological vulnerability, specifically, risk for pathologies characterised by premature brain senescence (Fig. 1, c-e). We reasoned that earlier timing of brain development/aging processes associated with short-term resilience in adolescence and middle adulthood could still reflect increased neurobiological "wear and tear" and, thus, be linked to cellular markers suggestive of long-term risk for accelerated brain aging pathologies.

Because history of exposure to stressors can impact short-term resilience (Kalisch et al., 2019), we sought to control for it through markers of key risk dimensions, such as deprivation (i.e., absence of expected environmental support [e.g., material, cognitive]), threat (i.e., actual or potential exposure to violence), and unpredictability (Colich et al., 2020; Ellis et al., 2022; McLaughlin et al., 2021). These dimensions overlapped the life domains assessed with the recent adverse events scales, specifically, financial difficulties, exposure to crime/physical violence, conflict, as well as unpredictable events involving interpersonal loss (e.g., [parental] separation/divorce) or other significant life changes (e.g., change of residence/school).

Our approach to controlling for prior stress exposure was grounded in evidence that dimensional operationalizations of adversity better capture long-term individual variability in neurodevelopmental outcomes relative to cumulative risk measures, which are further prone to recall biases, particularly for adult samples (Baldwin et al., 2019; Ellis et al., 2022; McLaughlin et al., 2021). Thus, the following indicators were used to estimate prior adversity exposure. First, global exposure to multiple dimensions of adversity was gauged through measures of socioeconomic status (SES) (Colich et al., 2020). Specifically, we used indices of income-to-needs, race and educational attainment, which reportedly encapsulate distinguishable experiential aspects relevant to deprivation (e.g., poverty [deprivation of vital material resources], reduced cognitive stimulation [cognitive deprivation]), threat (e.g., discrimination) and unpredictability (e.g., job insecurity) (Braveman et al., 2005; Colich et al., 2020; Machlin et al., 2019). Although individual- and/or family-focused, these measures (e.g., educational attainment) have been shown to be strongly correlated ($r >$ 0.50) with higher level environmental SES indicators, such as neighbourhood disadvantage (Murtha et al., 2022), which were unavailable in the Lifespan HCP dataset. Second, social environmental unpredictability was estimated through indices of marital relationship dissolution/reconfiguration ([parental] divorce/spousal death and the existence of step-parents, cf. Ellis et al., 2022), critical stressors across the lifespan (Kendler et al., 2017; Oh et al., 2018; Richards et al., 1997). Third, in the HCP-Development sample only, we further controlled for family conflict, a social threat-based stressor evaluated through both youth and parent ratings, which is a substantial contributor to psychological well-being in early life and has been linked to functional neurodevelopmental timing in late childhood/adolescence (Cummings and Miller-Graff, 2015; Harold and Sellers, 2018; Petrican et al., 2021). Fourth, likely exposure to physical violence/threat was quantified with a lifetime inventory of traumatic brain injury.

Accelerated biological aging pace was operationalised as earlier pubertal timing (HCP-Development) or more advanced menopausal status (HCP-Aging) than expected by chronological age. Brain maturation/senescence was estimated with both functional and structural indices since there is compelling evidence that the two can be differentially impacted by adversity (cf. Colich et al., 2020) and that uncoupling of normative developmental changes in structure and function may be detrimental (cf. Baum et al., 2020).

Our core neural marker was BOLD fMRI signal variability ($BOLD_{SV}$) due to its putative contribution to flexible and differentiated responding to the external milieu, its role in mediating environmental effects on long-term development and psychiatric risk, as well as its susceptibility to lifespan fluctuations (Cheng et al., 2021; Garrett et al., 2021; Grady and Garrett, 2018; Millar et al., 2020b; Nomi et al., 2017; Sheng et al., 2021; Wang et al., 2021). To capture mental state-specific effects (Waschke et al., 2021), $BOLD_{SV}$ was estimated during wakeful rest and during performance of an externally oriented inhibitory control task sensitive to developmental, adversity and psychopathology effects (Grahek et al., 2019; McTeague et al., 2017; Thompson et al., 2021; Tozzi et al., 2020; Vink et al., 2020).

BOLDsv is reportedly foundational to the development and maintenance of functionally segregated brain architecture, the linchpin of efficient and environmentally resilient processing, whose gradual emergence over the first two decades of life and subsequent decline from late middle-age onwards is accelerated though exposure to adversity (Baracchini et al., 2021; Chan et al., 2014; M.Y. 2018; Gabard-Durnam et al., 2016; Garrett et al., 2021; Geng et al., 2021; Grayson & Fair, 2017; Hughes et al., 2020; Soldan et al., 2021; Tooley et al., 2021;

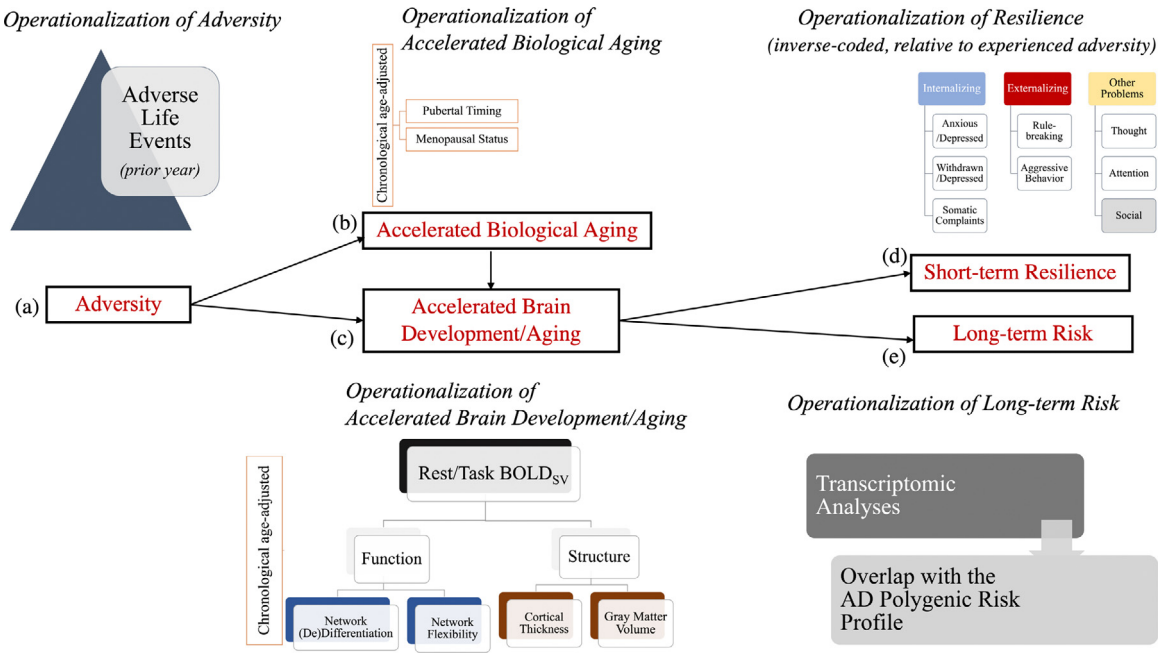

Fig. 1. Schematic representation of the conceptual/measurement model. Adverse life events were expected to accelerate brain development/aging, both directly (panels a-c), and via speeded biological maturation (panels a-b-c). This study focused on recent adversity (panel a) and sought to control for prior adversity exposure (see text). The goal was to identify patterns of accelerated brain development/aging linked to resilience (panels c-d) and probe their relevance to long-term psychological vulnerability, specifically, risk for pathologies characterised by premature brain senescence (panels c-e). Resilience (panel d) was operationalized as inverse coded total problems score on the Child Behavior Checklist (CBCL, HCP-Development) or on the Adult Self-Report (ASR, HCP-Aging) residualized for recently experienced adversity (in addition to the other confounders mentioned in the Method). Social problems are part of the total problems score only in the CBCL.

Sporns & Betzel, 2016). Relatedly, resting state BOLDsv is regarded as a reflection of generic priors that shape future behavioral responses (Pezzulo et al., 2021). As such, it is relevant to neurocognitive efficiency, operationalised as reduced task-resting state functional brain reorganization for similar behavioral performance levels (Heinzel et al., 2014; Neubauer and Fink, 2009). This capacity is linked to superior cognitive functioning (Schultz and Cole, 2016; Thiele et al., 2022), declines with age (e.g., greater task-rest reorganization in older adults, Hughes et al., 2020) and fluctuates with adversity exposure (Liu et al., 2021). Thus, in addition to $BOLD_{SV}$, indices of neurocognitive efficiency (i.e., reduced task-resting state functional flexibility) and specialization (i.e., resting state and task-related network differentiation) were tested for their relevance to psychological resilience.

To estimate structural neurodevelopmental timing, we focused on two morphological brain features, cortical thickness and gray matter volume (GMV). Both are robustly associated with $BOLD_{SV}$, possibly via synaptic pruning processes (Faust et al., 2021) and vary with age as a reflection of both typical and pathological cognitive changes (Giedd et al., 1999; Lindenberger and Lovden, 2019; Millar et al., a,b; Nadig et al., 2021; Pur et al., 2019; Roe et al., 2021; Sele et al., 2021; Vandekar et al., 2015). While meta-analytic evidence identifies cortical thickness as a critical indicator of adversity-induced accelerated neurodevelopment (Colich et al., 2020), a link between stress exposure and GMV is yet to be conclusively established. Nonetheless, across the lifespan, GMV fluctuations track with both short-term and long-term variations in circulating gonadal hormone levels (Herting et al., 2014; Kim et al., 2018; Rehbein et al., 2021). Consequently, we included GMV together with cortical thickness, reasoning that it could help explain biological aging effects on resilience-relevant brain profiles.

Finally, we examined whether the neural aging mechanisms underlying psychological resilience would be linked to molecular markers suggestive of increased long-term vulnerability to pathologies characterized by premature brain senescence (Cole et al., 2021; Dafsari and Jessen, 2020; Darrow et al., 2016; Fang et al., 2020; Han et al., 2021). We focused on Alzheimer's disease (AD), a condition robustly linked to stress exposure and accelerated cellular aging via low-grade systemic inflammation, whose onset is reportedly precipitated by earlier mood pathology (Beurel et al., 2020; Cao et al., 2021; Dafsari and Jessen, 2020; Darrow et al., 2016; Guerrero et al., 2021; Harerimana et al., 2022; Jin et al., 2021; Lutz et al., 2020; Ly et al., 2021; Riddle et al., 2017). To test the relationship between the neural substrates of short-term resilience and molecular markers of accelerated aging pathology, we used gene expression data from the Allen Institute of Brain Science. We thus estimated the overlap between the transcriptional signatures of our resilience-linked neural profiles and the AD polygenic risk profile derived from recent meta-analytic genome-wide association study (GWAS) results (Kunkle et al., 2019).

2. Method

2.1. Participants

The present research uses cross-sectional data preprocessed by the Lifespan HCP study team and downloaded in March 2021 as part of the 2.0 Data Release for the HCP-Development (www.hcp-development.org) and HCP-Aging (www.hcp-aging.org) studies. The two samples described below reflect the largest number of biologically unrelated participants who provided good quality data on all the variables of interest. We only included female participants because self-report measures of biological aging were unavailable for the males in the HCP-Aging sample. All participants were screened for a history of neurological, psychiatric, endocrine, genetic and other serious medical (e.g., diabetes, two or more seizures) disorders, use of psychotropic drugs, head injuries with loss of consciousness and/or change in mental functioning, and other conditions or bodily implants that may render their participation unsafe. Table 1 contains demographic information on both samples.

Table 1
Demographic Information for the HCP-Development and HCP-Aging Participants.

Variable	HCP-Development $N = 178$	HCP-Aging $N = 146$
Age (years)	12.27 ± 2.59	47.87 ± 7.03
Race (%White)	Caucasian (72.4%)	Caucasian (60.3%)
	African American (6.4%)	African American (21.2%)
	Asian (3.2%)	Asian (6.2%)
	Multiracial (16.9%)	Multiracial (7.5%)
	Not reported (1.1%)	Not reported (4.8%)
Family Income (USD) (adjusted for number of household members)	37,129 ± 30,864	45, 580 ± 57, 377
Education	Graduate School (39%);	Graduate School (34%);
	Four-/three-year college (38%);	Four-/three-year college (34%);
	One-/two-year college (10%);	One-/two-year college (23%);
	Highschool (13%)	Highschool (9%)
Handedness (% Mostly Right-handed)	92%	95%

Note. In the HCP-Development sample, education is that of the primary caregiver.

2.1.1. HCP-Development

This sample included 178 female participants, mostly right-handed ($N = 164$) and aged 8 to 18 years ($M = 12.27$ yrs, SD = 2.59 yrs). This age range was selected because it spans the various stages of pubertal development. The racial composition of the sample was as follows: White (72.4% [youth], 80% [parent/guardian]), African American (6.4% [youth] and 6% [parent/guardian]), Asian (3.2% [youth], 6% [parent/guardian]), mixed race (16.9% [youth], 6% [parent/guardian]) and unknown/unreported (1.1% [youth], 2% [parent/guardian]).

2.1.1.1. Additional exclusion criteria. Exclusion criteria specific to HCP-Development were premature birth and/or underweight birth weight, receiving special learning services at school and insufficient command of English to complete the study (for the youth and/guardian) (Somerville et al., 2018).

2.1.2. HCP-Aging

This sample encompassed 146 female participants, predominantly right-handed ($N = 139$) and aged 36 to 59 years ($M = 47.87$ yrs, SD = 7.03 yrs), an interval that captures the transition from reproductive to late post-menopausal status. The sample was 60.3% White, 21.2% African American, 6.2% Asian, 7.5% mixed race and 4.8% unknown/unreported.

2.1.2.1. Additional exclusion criteria. Exclusion criteria unique to the HCP-Aging were sensory (hearing/vision) deficits, uncontrolled high blood pressure, major organ failure, and Montreal Cognitive Assessment (MoCA) score of 19 or lower (Bookheimer et al., 2019).

2.2. Adversity

2.2.1. HCP-Development

The 25-item Adverse Life Events scale from the PhenX Toolkit (Stover et al., 2010) indexed participants' experience of negative events over which they which they had little control during the year preceding the study. The scale uses a *Yes/No* response format to gauge event occurrence, accompanied by a 4-point scale assessing event valence and a 6-point scale indexing event impact. Due to the low completion rate of the event rating scale, our analyses focused on the total number of adverse events experienced by the participants during the prior year. Of the 25 event items, we eliminated one that overlapped with our health covariates ("Got seriously sick or injured") and three that seemed likely to evoke heterogeneous affective responses across the sample ("Got new stepmother or stepfather", 'Parent got a new job", "Got new brother or sister"). The remaining event items reflected interpersonal loss (e.g., "Someone in family died"), interpersonal conflict (e.g., "Parents argued more than previously"), financial difficulties (e.g., "Mother/father figure lost job") or other life disruptions (e.g., "Family moved").

2.2.2. HCP-Aging

The 26-item Geriatric Adverse Life Events Scales (GALES, Devanand et al., 2002) gauged participants' experience of acute negative episodes during the year preceding the study. The instrument comprises a checklist of events, followed by 3-point ratings of event stressfulness and 6-point rating of event impact. Similar to the HCP-Development, the event rating scales had a low response rate, which is why our analyses included only the number of adverse events. As in the HCP-Development, we eliminated the two items that overlapped with health covariates ("New major physical illness","Other major physical illness"). We further excluded two items that diverged substantially from the life areas covered by the HCP-Development adverse events scale ("Difficulty getting adequate professional services", "Became caretaker for a friend/relative"). The remaining event items indexed life domains overlapping with those assessed by the corresponding HCP-Development event scale, specifically, interpersonal loss (e.g., death of a close other), interpersonal conflicts (e.g., divorce), financial difficulties (e.g., losing one's job) and other life disruptions (e.g., voluntarily changing place of residence).

2.3. Biological aging

2.3.1. Pubertal timing (HCP-Development)

Pubertal status was assessed with the 5-item Pubertal Development Scale (PDS), which was selected due to its significant correlation with other indices of pubertal development, including physician ratings (Petersen et al., 1988). The questionnaire comprises three gender-general items (i.e., growth spurt, changes in skin, hair growth) and two gender-specific items (e.g., breast development, menarche). The instrument, which uses a 4-point Likert type response format, ranging from 1 (no development) to 4 (development already completed), was completed by the youth if aged 9 and older and by the parent about the youth for the younger participants. The scale evidenced excellent reliability in the present sample (Cronbach's alpha = 0.87). An index of accelerated pubertal development was computed by regressing from the aggregate PDS score the youth's biological age, such that a positive residual score indicated accelerated biological aging (cf. Colich et al., 2020; Sumner et al., 2019).

2.3.2. Menopausal status (HCP-Aging)

Responses on the self-report survey Stages of Reproductive Aging Workshop (STRAW-10, Harlow et al., 2012) were used to estimate menopausal status, which is indexed with STRAW codes as "reproductive/premenopausal" (4.2), "late reproductive/premenopausal" (4.1), "early transition" (3), "late transition" (2), "early postmenopausal" (coded in chronological order as 1.11, 1.12, 1.13) and "late postmenopausal" (1.14). Participants who skipped periods due to reasons other than natural menopause (STRAW codes 2.20, 1.11002/4/7,

1.12002/4/7, 1.13002/4/7, 1.14002/4/7) were not included in the analyses. Menopausal status was estimated from the numerically transformed STRAW codes, which ranged in value from 1 ("reproductive age"/4.2) to 8 ("late postmenopausal"/1.14). Using data available from 126 of the 146 participants in our HCP-Aging sample and controlling for whether blood was collected after fasting, we verified that more advanced menopausal status was associated with higher levels of follicle stimulating hormone, Spearman's *rho* of 0.77, $p = .001$, and lower levels of estradiol, Spearman's *rho* of −0.58, $p = .001$ (cf. Harlow et al., 2012).

Biological aging was estimated by regressing out chronological age from the menopausal status index described above. Positive residual scores reflected accelerated, while negative scores implied decelerated, biological aging. We verified that age at menarche, a significant predictor of age at menopause, was not significantly associated with this index of biological aging, $r(144) = -0.10$, $p = .23$.

2.4. Resilience

In both samples, resilience was estimated by regressing out the number of adverse life experiences from the general psychopathology risk index (as described below) multiplied by −1. Positive residuals indicated greater, whereas negative residuals indicated poorer, resilience (i.e., better- vs. worse-than-expected psychological functioning given experienced adversity).

2.4.1. HCP-Development: Child Behavior Checklist (CBCL)

Psychological functioning was indexed with the parent-report version of the CBCL (Achenbach, 2009). This instrument was preferred to the Achenbach Youth Self-report Scale (YSR, Achenbach, 1991) because it ensured consistency across the developmental sample (i.e., the YSR is completed by participants aged 11 + years) and seemed likely to provide more reliable information for the younger adolescents. The CBCL consists of 112 items scored on a 3-point Likert scale (0 = *not true*, 1 = *somewhat or sometimes true*, 2= *very true or often true*). General psychopathology risk was quantified by using the raw Total Problems score made available in the Lifespan HCP 2.0 Data Release. This strategy is in line with Achenbach's (1991, 2013) recommendations that raw scores (rather than t-scores) be used in research given their greater precision particularly at the extremes of the scale. In our case, this was particularly appropriate since we used female-only samples and residualized for age in our analyses.

2.4.2. HCP-Aging: Achenbach Adult Self-Report Scale (ASR)

Participants' risk for psychopathology was assessed with the Achenbach Adult Self-Report (ASR) instrument for ages 18–59 (Achenbach, 2009). The ASR contains a total of 123 statements relevant to psychological functioning over the previous six months and, similar to the CBCL, it requires respondents to use a 3-point rating scale (0 = *not true*, 1= *somewhat or sometimes true*, 2 = *very true or often true*) to indicate how well each item described them. As in the HCP-Development sample, global psychopathology risk was estimated by using the raw Total Problems score, which, similarly to CBCL, is recommended for use in research over the adjusted t-score (cf. Achenbach, 1991, 2013).

2.5. Brain development/aging

2.5.1. In-Scanner task

Both samples completed a version of a classic Go/NoGo task, which juxtaposes free execution (Go trials) with inhibition (NoGo trials) of a preprotent motor response (Bookheimer et al., 2019; Davidow et al., 2019; Somerville et al., 2018; Winter & Sheridan, 2014). In the HCP-Development, the task stimuli were associated with a history of reward/punishment, an aspect that was omitted though in the HCP-Aging and, thus, for the sake of cross-sample comparability, also in our present analyses.

The task had an event-related design and required participants to press a button as soon as possible after seeing one of six shape stimuli (Go trials), but refrain from making a response to a circle or square (NoGo trials). Each shape was presented for 600 ms with a variable inter-trial interval of 1 to 4.5 s. To minimize predictability, NoGo trials are separated by 2, 3 or 4 consecutive Go trials. Go trials were marked as correct if a button press was made within the response window (i.e., 600 ms stimulus presentation and 200 ms into the subsequent fixation interval), whereas the converse applied to NoGo trials. In both samples, each task run contained 24 NoGo trials and 68 Go trials.

2.5.2. Data acquisition

Scanning was performed across 4 US sites on Siemens Prisma 3T scanners (32-channel coil; for details, see Harms et al., 2018). T1-weighted images were acquired with a multi-echo MPRAGE sequence with the following parameters: TR=2500, TE = 1.8/3.6/5.4/7.2 ms, flip angle=8°, FOV = 256 × 240 × 166 mm, 320 × 300 matrix, 208 slices, 0.8 mm isotropic voxels. The fMRI data were acquired with a multiband gradient-recalled (GRE) EPI sequence (TR=800 ms, TE=37 ms, flip angle=52°, FOV = 208 mm, 104 × 90 matrix, 72 oblique axial slices, 2 mm isotropic voxels, multiband acceleration factor of 8).

Four rfMRI scans (eyes open with passive crosshair viewing), lasting 26 min in total, were collected from all the participants included in the present report. Two rfMRI scans were acquired with an anterior-to-posterior (AP) and the other two with a posterior-to-anterior (PA) phase encoding sequence. Because HCP-Aging included only one scan per task, our analyses of the inhibitory control data are based on the corresponding PA task run collected from each sample (4:11 min) (Harms et al., 2018).

2.5.3. Data preprocessing

The main processing steps applied to these data by the HCP study team are outlined below (for further details on specific steps, see Glasser et al., 2013; Robinson et al., 2018). Using the "fmriresults01" file, available for each of the two samples as part of the 2.0 Data Release, we confirmed that the structural and functional outputs of the preprocesssing pipelines described below passed the quality control checks implemented by the HCP team.

2.5.3.1. sMRI. The sMRI data were processed with the HCP Structural Pipelines (Pre-FreeSurfer, FreeSurfer, Post-FreeSurfer). The Pre-FreeSurfer pipeline included removal of non-brain tissue, corrections for gradient non-linearity distortions and intensity inhomogeneity, as well as intensity normalization. The FreeSurfer pipeline (http://surfer.nmr.mgh.harvard.edu/) generated the surface and volume anatomical parcellations, as well as morphometric measurements of structure volumes and surface areas (cf. Dale et al., 1999; Fischl et al., 2001, 2002, 1999a; Fischl et al., 1999b). The Post-FreeSurfer pipeline transformed the FreeSurfer outputs to NIFTI or GIFTI formats, applied the transforms generated with the Pre-FreeSurfer pipeline to bring the structural images into the standard Montreal Neurological Institute (MNI)−152 template (0.8 mm isotropic voxels), projected the subject's native mesh surfaces into standard mesh surfaces (164k_fs_LR/32k_fs_LR) and generated surface myelin maps and ribbon volume myelin maps. The structural data thus processed were subsequently precisely aligned across participants through multimodal surface mapping (MSM) registration which combines information regarding sulcal depth, myelin and functional connectivity patterns in order to optimize registration of functional cortical areas across subjects (Robinson et al., 2018).

2.5.3.2. fMRI. The fMRI data were processed by applying the Generic fMRI Volume and Surface Processing Pipelines, multi-run independent component analysis (ICA) FIX denoising and multimodal surface matching registration. The Generic Volume Processing Pipeline accomplished removal of spatial and gradient distortions, correction for participant

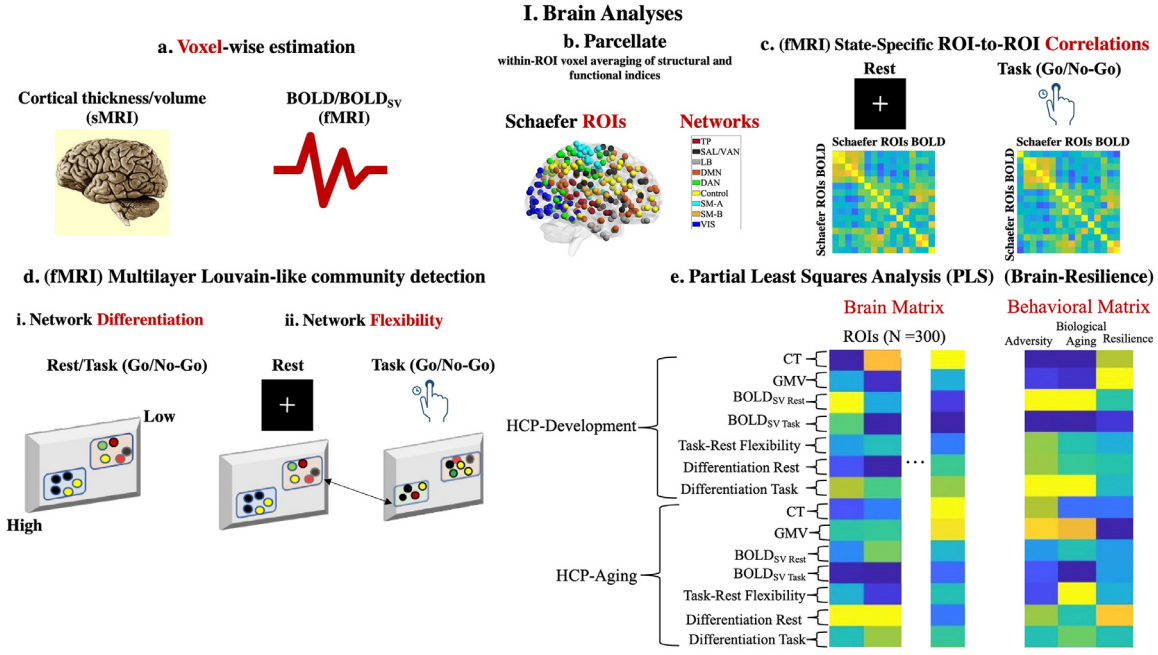

Fig. 2. Schematic representation of the brain(-behavior) analysis pipeline described in the Method. Voxel-wise structural and functional indices (panel a) were averaged within each of the 300 ROIs from the Schaefer Atlas (panel b). To increase comparability with the Gordon atlas, results for the sub-components of the Schaefer networks are not presented separately apart from the somatomotor A and somatomotor B networks (panel b) which map onto the somatomotor-hand and somatomotor-mouth networks from the Gordon atlas. Pairwise correlations in the timeseries of all 300 Schaefer ROIs were estimated as Fisher's z-transformed scores (panel c). Positive z-transformed scores were inputted into a multilayer Louvain-like community algorithm to quantify ROI-based indices of functional network differentiation during rest and a Go/No-Go task, as well as indices of task-rest functional flexibility (panel d). Following residualization for confounds (non-imaging variables only, see text), the ROI-specific structural and functional indices, as well as measures of adversity exposure, biological aging and psychological resilience were entered into a partial least squares (PLS) analysis (panel e). CT = cortical thickness. GMV = gray matter volume. (For interpretation of the references to colour in this figure legend, the reader is referred to the web version of this article.)

movement, bias field removal, spatial normalization to the standard Montreal Neurological Institute (MNI)−152 template (2 mm isotropic voxels), intensity normalization to a global mean and masking out of non-brain voxels. Subsequent temporal preprocessing steps involved weak high-pass temporal filtering with the goal of removing linear trends in the data. The Generic Surface Processing Pipeline registered the functional data into a standard grayordinate space by projecting the cortical gray matter into a registered surface mesh with a standard number of vertices (32k_fs_LR mesh) and projecting the subcortical data to a set of subcortical gray matter voxels. A small amount of spatial smoothing (2 mm full-width-at-half-maximum [FWHM]) was also applied to the functional data at this step. The ICA FIX denoising pipeline, which combines FSL's MELODIC with a more complex automated noise identifier ("FIX"), handled removal of artifacts (e.g., rigid/physiological motion-related) which had survived the Generic fMRI Volume Preprocessing step (for details, see Griffanti et al., 2014). Finally, similar to the structural data, the cleaned functional data were precisely aligned across participants through MSM registration (Robinson et al., 2018).

2.6. Data analysis

Our pipeline is depicted in Fig. 2 and the main steps are described below.

2.6.1. ROI definition

Our main analyses were based on the Schaefer 300 parcel-functional atlas (Schaefer et al., 2018; Yeo et al., 2011), downloaded from https://github.com/ThomasYeoLab/CBIG. The atlas version we used encompasses 17 functional networks, spanning core systems, such as the DMN (A/B/C), Control (A/B/C), Salience/Ventral Attention (A/B), Dorsal Attention (DAN A/B), Somatomotor (SM A/B), Visual (VIS Central/Peripheral), Limbic (LB A/B), and Temporo-parietal (TP). To test whether age would impact intrinsic ROI functional homogeneity, we estimated the standard deviation (SD) in resting state BOLD signal across all the component voxels within each ROI at each time point using the "cifti-parcellate" command with the STDEV method in the Connectome Workbench. A Mann-Whitney test provided evidence of significantly greater ROI functional inhomogeneity in the HCP-Aging relative to the HCP-Development (Mdns of 101.56 and 113.80, *U (standardized test statistic)* = 11.21, p = .0001). Consequently, to account for inter-individual differences in how well the Schaefer functional brain atlas fit the present data, our SD-based measure of functional homogeneity, averaged across all ROIs and time points, was regressed out from all the neuroimaging variables of interest (see Section 2.7 below).

2.6.2. BOLD$_{SV}$

Based on the Schaefer atlas, ROI-level standard deviations in BOLD signal were computed separately for the rest and for the inhibitory control task run (Garrett et al., 2020, 2010). These calculations were based on fully preprocessed functional data (as described above).

2.6.3. BOLD$_{SV}$-related morphological characteristics

FSL's FAST was applied to each participant's MNI aligned T1 images in order to obtain voxelwise gray matter volume (GMV) estimates. Subsequently, GMV estimates were extracted for each of Schaefer ROIs using fslmeants. Likewise, based on the corresponding MSM registered 32k_fs_LR .dscalar.nii files, ROI-specific cortical thickness estimates were obtained using the Schaefer .dlabel.nii atlas files and the "cifti parcellate" function in the Connectome Workbench.

2.6.4. BOLD$_{SV}$-related functional architectural features

To test our hypotheses regarding the indirect contribution of BOLD$_{SV}$ to psychological resilience via functional network differentiation and

flexibility across multiple mental states, we conducted the connectivity analyses detailed below.

2.6.4.1. ROI-to-ROI correlations in timeseries. Pairwise Pearson's correlations between all the Schaefer ROIs were computed separately for task and rest in Matlab and expressed as Fisher's z-transformed scores. Previous research has documented differences in the brain's modular organization (i.e., number of identified communities) based on the time scale on which connectivity has been assessed (Bassett et al., 2011). To avoid having time scale act as a potential confound when comparing task-rest functional brain organization, we opted to characterize resting state connectivity on the same time scale as task-related connectivity, thereby breaking the 1912-volumes resting state data into six blocks of 290 vol each (the additional volumes from the beginning and end of the resting state scan were dropped from the analyses). In line with prior studies using multilayer community detection algorithms (e.g., Finc et al., 2020), only the positive Fisher's z-scores were entered in the network-level analyses detailed below, while negative z-scores were set to zero.

2.6.4.2. Network-level analyses. All the network-level metrics were computed using the Brain Connectivity Toolbox (BCT, Rubinov & Sporns, 2010) and the Network Community Toolbox (NCT, Bassett, D.S. [2017, November]. Network Community Toolbox. Retrieved from http://commdetect.weebly.com/), as described below.

2.6.4.2.1. Functional community structure: multilayer louvain-like algorithm. To characterize patterns of ROI-based functional reorganization between rest and task, we used a multilayer generalised Louvain-like community detection algorithm, first introduced by Mucha et al. (2010) and implemented in the NCT. This algorithm partitions a network with multiple layers into non-overlapping groups of nodes (i.e., functional communities) with the goal of maximizing an objective modularity quality function, defined as

$$\mathbf{Q} = \frac{1}{2\mu}\sum_{ijlr}\left[\left(w_{ijl} - \gamma_l e_{ijl}\right)\delta_{lr} + \delta_{ij}\omega_{jlr}\right]\delta\left(g_{il}, g_{jr}\right)$$

where 2μ is the sum of all connection weights in the network across all layers, w_{ijl} represents the connection strength between nodes i and j in layer l; γ_l is a resolution parameter determining the size of the identified modules in layer l; e_{ijl} is the connection strength expected by chance between nodes i and j in layer l, and defined as $e_{ijl} = \frac{s_{il}s_{jl}}{v}$ with s_{il} and s_{jl} being the sum of all connection weights of node i and j, respectively, in layer l, while v is the sum of all connection weights in the network in layer l; ω_{jlr} is the connection strength between node j in layer l and node j in layer r, and g_{il} and g_{jr} give the community assignments of node i in layer l and node j in layer r.

In the above modularity quality optimization, there are two free parameters, the spatial resolution parameter, γ, which tunes community size within each layer, and the cross-layer connection strength parameter, ω, which determines community stability across layers. In our study, the two network layers were defined by the rest and the inhibitory control task, respectively. Dovetailing with the prior literature (Finc et al., 2020; Mattar et al., 2015), the spatial resolution parameter was set to the default value of 1. In line with other studies of heterogenous mental states (Finc et al., 2020), the cross-layer (task-rest) connection strength parameter was set to 0.5. To account for the near degeneracy of the modularity landscape (Good et al., 2010), the multilayer community detection algorithm was initiated 100 times for each of the six task-rest pairs (as described above, the rest scan was broken down into six blocks equal in duration to the task block). All the functional network interactions indices detailed below were averaged across the 600 iterations of the modularity optimization function (6 task-rest pairs x 100 iterations/pair).

2.6.4.2.2. Functional network interactions. Our analyses focused on two ROI-level functional interaction diagnostics, which were computed in the NCT across the 600 iterations of the multilayer community detection algorithm: (1) functional flexibility/task-resting state functional reorganization, operationalised as the number of times each ROI in the Schaefer atlas changed communities between task and rest, and (2) differentiation/segregation (called "recruitment" in the NCT), which was estimated separately for task vs rest, and operationalised as the number of times a given ROI was assigned to the same community as the other ROIs in its native functional system, as defined in the Schaefer functional atlas. To facilitate mapping of the relevant results onto the conceptual model presented in Fig. 1, indices of functional network differentiation during task and rest were multiplied by −1 in the HCP-Aging sample, so that higher scores would reflect greater dedifferentiation consistent with greater functional brain aging. This was done post-analysis for presentational purposes only.

2.7. Confounding variables

2.7.1. Family conflict

The 9-item Family Conflict subscale of the Moos Family Environment Scale (Moos and Moos, 1994) gauged exposure to domestic violence in the HCP-Development sample. Each item is scored as *1* or *0* for *true/false*, with reverse coding of items that imply lack of conflict in the home (e.g., "We fight a lot in our family." versus "Family members rarely become openly angry."). Higher scores indicate a more conflictual family environment. Both parent and youth versions demonstrated acceptable reliability (Cronbach's alphas of 0.67 and 0.61). Two parents and one youth failed to answer one item on the scale. Consequently, for both caregiver and youth versions, all the reported analyses used the sum scores prorated by number of missing items, as available in the Lifespan HCP 2.0 Data Release. Consistent with the interpretation that youth and parent evaluations may capture distinguishable aspects of the family environment, the two scores were only moderately correlated, Spearman's *rho* of 0.28, $p = .0001$. We opted to control not only for youth, but also parental measures of conflict because the latter could capture indirect routes through which interpersonal conflict which did not involve the youth may have still impacted their psychological functioning.

2.7.2. Residualization

Recent literature suggests that residualization of both variable sets introduced in multivariate analyses such as PLS or canonical correlation analyses , which use permutation-based significance testing, may bias results (Winkler et al., 2020). Consequently, we only residualized the non-imaging variables entered in the PLS analyses (i.e., recently experienced adversity, biological aging, resilience). All residualization analyses were conducted separately in the HCP-Aging and HCP-Development samples. The following confounders were thus regressed out from each of the three non-imaging variables using multiple linear regression analysis:

(1) participants' chronological age in order to estimate accelerated/decelerated development/aging and recent adversity exposure independent of age (within each group),
(2) SES indicators: (a) race (represented through four dummy coded variables "African American","Asian", "Multiracial", "Not Reported") which also accounted for racial differences in genetic architecture and risk loci (Abdellaoui and Verweij, 2021; Nievergelt et al., 2019; Wojcik et al., 2019) potentially relevant to adversity exposure and psychological resilience; (b) income-to-needs (i.e., family income divided by number of dependants, see Table 1); (c) educational attainment (of the primary caregiver in HCP-Development [to ensure consistency across participants given variability in parental marital status and availability of educational information for the second biological parent/primary caregiver's current partner] and of the participant in HCP-Aging, coded as a continuous variable, see Table 1),
(3) history of social environmental unpredictability predating the prior year: sum of parental divorce and having a step-parent (maximum possible value of "2", HCP-Development) or number of divorces and/or times one has been widowed (HCP-Aging);

(4) chronic social threat: family conflict (HCP-Development only, youth and parent ratings),
(5) history of likely exposure to physical threat/violence: (HCP-Aging only) lifetime history of head trauma (cf. Saikumar and Bonini, 2021) based on the total score from the Boston Assessment of Traumatic Brain Injury-Lifetime Questionnaire (Fortier et al., 2014; the sole HCP-Development participant relevant to our objectives with head trauma followed by loss of consciousness was eliminated from analyses),
(6) physical health outcomes potentially also linked to prior adversity exposure and which could have impacted the neuroimaging measures (all scores available in the 2.0 Data Release): (a) BMI (coded as a continuous variable), (b) regular medication use (dummy coded as Yes/No),
(7) handedness (continuous) score,
(8) scanner site (three dummy variables [i.e., "Harvard"[HCP-D*evelopment*]/"Massachusetts General Hospital"[HCP-Aging] coded "1″ for participants tested at Harvard/ Massachusetts General Hospital and "0″ otherwise, "Minnesota" coded "1″ for participants tested at the University of Minnesota and "0″ otherwise, "UCLA" coded "1″ for participants tested at UCLA and "0″ otherwise; Washington University in St. Louis was the baseline against which the other three sites were compared) to account for broad demographic and individual scanner-related differences among sites),
(9) participant-specific average SD in resting state BOLD signal across all voxels within each ROI at each time point as a participant-specific index of "brain fit" with the Schaefer functional atlas,
(10) average scan-specific motion per participant (Power et al., 2015),
(11) overall accuracy on the SST operationalised as sum of misses on the Go trials and false alarms on the No-Go trials in order to capture individual differences in *how* the participants managed the task demands irrespective of their behavioral performance.

2.7.2.1. Data reduction: multivariate normality. The multiple linear regression analyses used for confounder residualization are sensitive to violations of multivariate normality (Hair et al., 2014), which we observed in our original data. To address this issue, a square-root transformation was applied to the Total Problems scores in both samples prior to residualization for confounders. In the HCP-Development sample, issues of multivariate non-normality further required elimination of a univariate outlier on recent adversity (z-score > 4) and elimination of multivariate (Mahalanobis distance-based, $p < .001$) outliers prior to residualization, leaving a final sample of 168 participants. Following these steps, an examination of the adversity, resilience and accelerated biological aging residuals using the Kolmogorov-Smirnov test (with the Lilliefors significance correction) confirmed that multivariate non-normality issues had been solved in both samples (all ps > 0.05).

2.8. Brain-behavior-gene analyses

2.8.1. Partial least squares analysis (PLS)

To identify brain patterns linked to adversity, resilience and biological aging, as well as characterize the relationship between brain and gene expression profiles, we used partial least squares correlation often referred to as *PLS* (Krishnan et al., 2011), a multivariate technique that can identify in an unconstrained, data-driven manner, neural patterns (i.e., latent variables or LVs) related to different conditions (i.e., task PLS) and/or individual differences variables (behavioral PLS). PLS was implemented using a series of Matlab scripts, which are available for download at https://www.rotman-baycrest.on.ca/index.php?section=345.

2.8.1.1. Brain differences related to adversity, biological aging and resilience: behavioral PLS 1. To identify yoked differences in profiles of brain morphology and function, which are linked to adversity, biological aging and resilience, we conducted one behavioral PLS analysis in which each data type was modelled as a separate condition. Number of adverse events, accelerated biological aging, resilience—all of which had been residualised for confounders as described above and, thus, presented themselves as approximate continuous Gaussian variables—were entered as the behavioral variables. The HCP-Development and HCP-Aging participants were entered as two separate groups. By entering the two groups in the same analysis we were able to probe age group-specific vs age group-independent brain correlates of adversity, accelerated biological aging, and resilience.

2.8.1.2. Gene expression-brain profile associations indicative of risk vs resilience: behavioral PLS 2. A behavioral PLS analysis probed the link between gene expression profiles and patterns of brain structure/function relevant to adversity and resilience. The latter was the brain LV identified in behavioral PLS analysis 1. The former was expressed as an ROI x gene expression level matrix and derived with the abagen toolbox from the comprehensive transcriptomic maps provided by the Allen Brain Institute (see section "Gene Expression Data Processing and Analysis" below).

2.8.1.3. Significance and reliability testing. In all the reported PLS analyses, the significance of each LV was determined using a permutation test (5000 permutations for the brain-[behavior] analyses and 100,000 permutations for all the analyses involving gene expression data). In the permutation test, the rows of the ROI or of the gene expression data are randomly reordered (Krishnan et al., 2011). In all PLS analyses, potential axis rotations (i.e., changes in the order of the extracted LVs) and reflections (i.e.,changes in the sign of the saliences), which may occur during resampling with either permutations or bootstrapping, were corrected with a Procrustes rotation, which defines a transformation through which the resampled singular value decomposition outcome (i.e., the identified LVs) is rotated to match most closely the original singular value decomposition outcome (Milan and Whittaker, 1995).

In the gene-brain PLS analysis, to account for correlated gene expression patterns based on anatomical proximity (Fornito et al., 2019; Markello & Misic, 2021) we used Vasa's "rotate_parcellation" function in Matlab (https://github.com/frantisekvasa/rotate_parcellation/commit/bb8b0ef10980f162793cc180cef371e83655c505) in order to generate 100,000 spatially constrained permutations of the Schaefer brain LV, as identified in behavioral PLS analysis 1. These spatially constrained permuted brain LVs were used to assess the significance of the extracted gene LVs.

In the case of our present analyses, PLS assigned to each ROI or gene a weight, which reflected the contribution of the respective ROI or gene to a specific LV. The reliability of each ROI's or gene's contribution to a particular LV was tested by submitting all weights to a bootstrap estimation (1000 bootstraps for the brain-[behavior] analyses and 100,000 bootstraps for all the analyses involving gene expression data) of the standard errors (SEs, Efron, 1981) (the bootstrap samples were obtained by sampling with replacement from the participants, Krishnan et al., 2011). In order to increase the stability of the reported results, we used a number of permutations/bootstraps several orders greater than the standard ones (i.e., 500 permutations/100 bootstrap samples), as recommended by McIntosh and Lobaugh (2004) for use in PLS analyses of neuroimaging data. The higher number of permutations/bootstraps used for the gene expression data was determined by the relatively lower result stability compared to the brain-(behavior) only analyses, as suggested by preliminary successive iterations of the gene PLS analysis using 5000 permutations/1000 bootstraps. A bootstrap ratio (BSR) (weight/SE) of at least 3 in absolute value (approximate associated p-value of .0027) was used as a threshold for identifying those ROIs that made a significant contribution to the identified LVs. For the gene PLS analyses, we focused on approximately the top 20% of absolute value BSRs (i.e., approximately top 10% at either tail of the distribution), which amounted to a BSR at least 5 (approximate associated p-value < 10^{-5}). The BSR is analogous to a z-score, so an absolute value greater than 2 is thought to

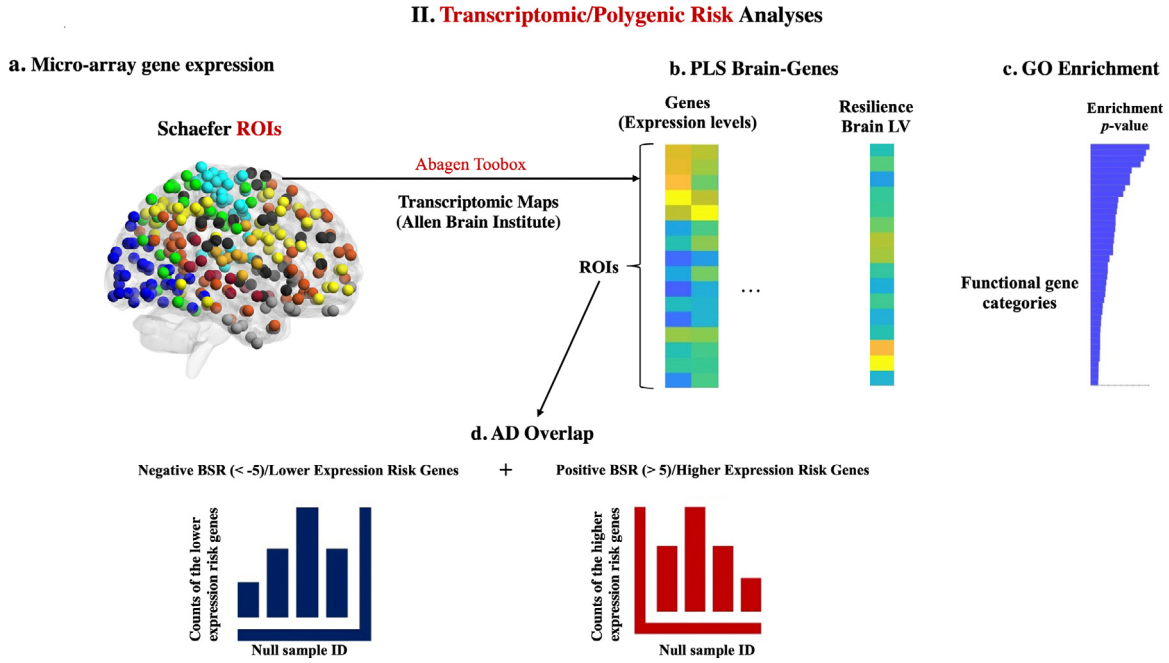

Fig. 3. Schematic representation of the transcriptomic and polygenic risk data analysis pipeline described in the Method. Micro-array gene expression data provided by the Allen Brain Institute were inputted into the abagen toolbox in order to estimate gene expression levels for each of the Schaefer ROIs (panel a). A PLS analysis was conducted on the ROI-specific gene expression data and the brain LVs linked to adversity and resilience in order to identify their transcriptional signatures (panel b). A GO enrichment analysis was performed to identify the functional gene categories associated with the resilience brain LVs (panel c). Permutation-based testing (see main text) was used to characterize the overlap between the gene expression profile relevant to resilience and the AD risk genes identified in prior meta-analyses (panel d). In panel (d) we illustrate the estimation of AD risk for cases in which the brain LV of interest is positively correlated with the identified gene LV (as per panel b). AD = Alzheimer's Disease. LV = latent variable. PLS = partial least squares analysis. GO = gene ontology.

make a reliable contribution to the LV (Krishnan et al., 2011), although for neuroimaging data BSR absolute values greater than 3 tend to be used (McIntosh & Lobaugh, 2004).

2.8.2. Mediation analyses

To test potential mechanisms through which neurodevelopmental timing may mediate the impact of adversity on psychopathology, we used Hayes' PROCESS 3.5 macro for SPSS (Hayes, 2018). PROCESS is an ordinary least squares (OLS) and logistic regression path analysis modeling tool, based on observable variables. Mediation models were tested employing 95% confidence intervals with 50,000 bootstrapping samples. In line with extant guidelines on balancing Type I and Type II errors in mediation analyses (Hayes and Scharkow, 2013; Tofighi and Kelley, 2020), the confidence intervals for indirect effects was estimated using percentile bootstrap, which is the default option in PROCESS 3.5. As recommended by Hayes and Cai (2007), a heteroskedasticity consistent standard error and covariance matrix estimator was used. Bootstrapping-based 95% confidence intervals for the indirect effects, as outputted by PROCESS, were used as effect size estimates. In the mediational analyses, number of adverse events experienced in the prior year constituted the predictor variable, whereas global psychopathology (i.e., raw Total Problems score) representated the main outcome. Profiles of accelerated/decelerated brain development/aging, linked by PLS to adversity and/or psychological resilience, were tested as potential mediators.

2.8.3. Gene expression data processing and analysis

Fig. 3 depicts the pipeline for the transcriptomic and polygenic risk data analyses. The main steps are described below.

2.8.3.1. Microarray gene expression. Micro-array gene expression data were obtained from six postmortem brains (1 female, ages 24.0–57.0, 42.50 +/- 13.38) provided by the Allen Institute for Brain Science (https://www.brain-map.org/). Because only two of the six brains contained data from the right hemisphere and gene expression patterns are largely symmetric across the two hemispheres, our main analyses were based on gene expression patterns mirrored across the two hemispheres. However, we also verified that the results of our gene enrichment AD-related gene expression analyses are replicated when only using gene-brain data from the left hemisphere ROIs (cf. Ball et al., 2020; Hansen et al., 2021; see Supplementary Materials). The gene expression data was processed with abagen (https://github.com/netneurolab/abagen). Microarray probes were re-annotated based on the probe-to-gene mapping information provided by Arnatkevičiūtė et al. (2019) and filtered based on their expression intensity relative to background noise (Quackenbush, 2002), such that probes with intensity less than the background in >=50% of samples across donors were discarded. When multiple probes indexed the expression of the same gene, we selected and used the probe with the most consistent pattern of regional variation across donors (i.e., differential stability; Hawrylycz et al., 2015).

The MNI coordinates of tissue samples were updated to those generated via non-linear registration using the Advanced Normalization Tools (ANTs; https://github.com/chrisfilo/alleninf). Samples were assigned to brain regions in the Schaefer atlas if their MNI coordinates were within 2 mm of a given parcel. All tissue samples not assigned to a brain region in the provided atlas were discarded.

Inter-subject variation was addressed by normalizing tissue sample expression values across genes using a robust sigmoid function (Fulcher et al., 2013):

$$x_{norm} = 1/\left(1 + \exp\left(-(x - \langle x \rangle)/\mathrm{IQR}_x\right)\right)$$

where $\langle x \rangle$ is the median and IQRx is the normalized interquartile range of the expression of a single tissue sample across genes. Normalized expression values were then rescaled to the unit interval:

$$x_{scaled} = \left(x_{norm} - \min\left(x_{norm}\right)\right)/\left(\max\left(x_{norm}\right) - \min\left(x_{norm}\right)\right)$$

Gene expression values were then normalized across tissue samples using an identical procedure. Samples assigned to the same brain region were averaged separately for each donor and then across donors. After we eliminated the ROIs without reliable gene expression (based on the abagen parameters outlined above), the resulting gene expression matrix, used in all our analyses, was in the format 297 (ROIs) x 15,632 (genes). A list of ROIs lacking reliable gene expression is included in the Supplemental Materials (Table S1).

2.8.3.2. Gene ontology (GO) enrichment analysis. To identify the functional gene categories that underpin the link between the resilience-relevant brain and the gene expression profiles, we used the software toolbox created by Fulcher et al. (2021). This toolbox has been shown to adequately control for within gene ontology (GO) category gene-gene co-expression patterns, thereby mitigating the potential for inflated false positive rates which can affect traditional inference methods of GO enrichment. Enrichment analyses were conducted using 40,000 custom null ensembles, obtained by using Vasa's algorithm to rotate the resilience-linked brain LVs from behavioral PLS analysis 1. Analyses were conducted on GO categories comprising 5 to 200 genes. Below we report the corrected *p*-values obtained by fitting a Gaussian distribution to the estimated null distribution.

2.8.3.3. AD overlap tests. To probe the link between short-term psychological resilience and longer-term risk for accelerated cognitive aging pathologies, we examined the overlap between our resilience-relevant gene expression LV and AD risk genes identified in prior meta-analyses of genome-wide brain association studies (GWAS, minpGWAS of at least 10^{-7}, Kunkle et al., 2019). The AD-relevant candidate risk loci had been mapped onto the corresponding genes by the original authors using the SNP2GENE tool in FUMA and made available via the *Public Results* tab (https://fuma.ctglab.nl/browse, Watanabe et al., 2017). Based on their eQTL analysis output, we identified 77 AD-linked genes reliably expressed in our data. Of these, the risk allele(s) reduced gene expression for 44 of them (*AD_low*), but increased gene expression for the remaining 33 (*AD_high*).

2.8.3.3.1. Resilience-relevant gene LV. Our AD risk overlap tests were conducted on genes with an absolute value BSR of at least 5 (associated *p*-value $< 10^{-5}$). Comparisons were conducted separately for genes with positive versus negative loadings on the gene LV. As an example, for the positive BSR genes, the procedure was as follows: (1) we obtained separate counts of the number of *AD_low* and *AD_high* genes, respectively, with a BSR of at least 5 on our gene LV (*AD_low_pos* and *AD_high_pos*, respectively); (2) we counted the number of genes with a BSR of at least 5 on our gene LV (*Orig_pos*); (3) from each of the corresponding gene LVs in the null distribution (each of which had been aligned with the original gene LVs via a Procrustes transform), we selected a number of genes equal to *Orig_pos* (*Null_pos*); (4) we counted the number of null samples (out of the total of 100,000) in which the number of either *AD_low_pos* or *AD_high_pos* in *Null_Pos* exceeded the one observed in *Orig_pos*. The same procedure was followed for the negative BSR genes. The estimation of the AD risk associated with a given brain LV depended on the sign of the correlation between the gene and brain LV. For instance, if the identified gene LV were to be positively correlated with the brain LV of interest, then the associated AD risk would be estimated as a conjunction of *AD_low* genes with negative BSRs and *AD_high* genes with positive BSRs observed in the original data relative to the null distribution.

2.9. Replication of results

All the results reported below were replicated using bi-hemispheric data from the Gordon atlas (Gordon et al., 2016), as well as left-hemisphere-only data from the Schaefer and Gordon atlases, respectively (for results of these analyses, see Supplemental Materials). The left-hemisphere only analyses were solely relevant to the brain-gene analyses and were conducted to verify the robustness of our bi-hemispheric results, because only two of the six donors from the Allen Brain Institute had right hemisphere transcriptomic data. Furthermore, because operationalization of racial ancestry can be difficult and its interpretation open to some debate (e.g., whether it reflects genetic vs SES-related effects), we further replicated all the results in analyses in which we did not control for racial background. In the Results below, based on the Schaefer atlas, we only discuss the results replicated across all the control analyses outlined above and included in the Supplemental Materials. These results are presented in red rectangles in Figs. 4 and 5.

3. Results

3.1. Brain profiles linked to adversity and resilience: behavioral PLS analysis 1

This analysis identified two LVs (both *ps* = 0.0002), accounting for 25.20% (LV1) and 12.14% (LV2) of the brain-behavior covariance.

3.1.1. LV1: accelerated functional brain development/aging correlates with recent exposure to adversity in adolescence and middle age

LV1 reflected primarily brain patterns linked to adversity exposure and was most robustly expressed in ROIs from the DMN, SAL-VAN, Control, DAN, SM and VIS (see Fig. 4-a and Table S2). In both samples, this LV reflected the positive association between recent adversity exposure and accelerated functional brain development (i.e., increased task-related network differentiation, HCP-Developmment, Fig. 4-b) or aging (i.e., reduced $BOLD_{SV}$ during both task and rest, HCP-Aging, see Fig. 4-c). Furthermore, in both adolescence and middle adulthood, the adversity-linked profile of earlier functional brain development/senescence was also associated with accelerated biological aging. Supplemental analyses replicating these results are presented in Figures S1, S3, and S5.

3.1.2. LV2: opposing patterns of functional brain development/aging involving SM, control, dmn and sal-van predict resilience in adolescence versus middle adulthoodhood

LV2 differentiated developmental/aging patterns observed in DMN and SAL-VAN ROIs from those detected in SM and Control ROIs (see Fig. 5-a, b and Table S3). In the HCP-Development sample, this LV linked greater resilience, recently experienced adversity and faster biological aging to accelerated SM and Control, but delayed DMN and SAL-VAN, functional development, as indicated by patterns of $BOLD_{SV}$ and functional network differentiation (see Fig. 5-c). Complementarily, in the HCP-Aging sample, LV2 associated higher levels of resilience, recently experienced adversity and slower biological aging with delayed SM/Control, but accelerated DMN/SAL-VAN functional aging, as reflected in patterns of functional network dedifferentiation and task-resting state topological flexibility (see Fig. 5-d). These results were replicated in the corresponding supplemental analyses (see Figures S2, S4, and S6).

3.2. Functional brain mechanisms protecting against adversity-linked psychopathology: mediation analyses

Based on our proposed neural sequence related to psychological resilience (Fig. 1-c), we next tested the role of $BOLD_{SV}$ and of its putative functional network correlates (task-rest flexibility, task/rest differentiation) in partially accounting for the shared variance between adversity and psychopathology. No structural brain variables were included in these analyses since none evidenced robust relationships with either resilience or adversity in the PLS analyses. Based on the PLS-identified brain LVs linked to adversity exposure and resilience (and replicated in the supplemental analyses), our mediation analyses focused on LV2

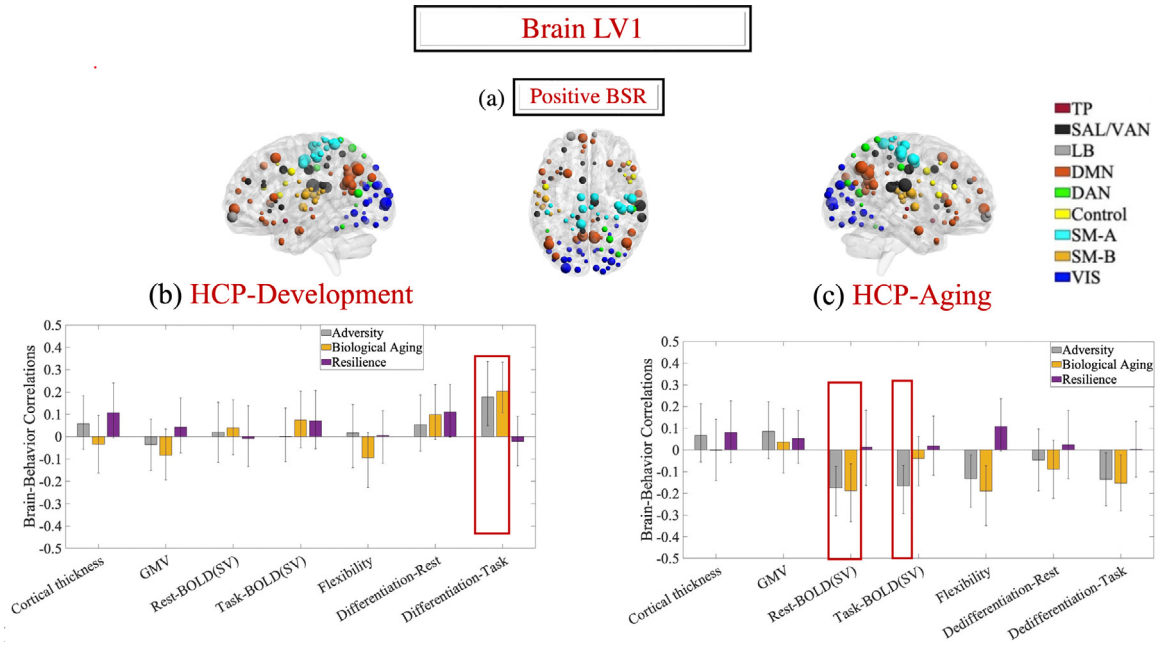

Fig. 4. First extracted LV from the behavioral-PLS analysis linking adversity and biological aging to brain maturation (HCP- Development) or senescence (HCP-Aging). Panel (a) depicts the Schaefer ROIs with robust loadings (absolute value BSR > 3) on the LV in panels (b, c) and visualized with the BrainNet Viewer (http://www.nitrc.org/projects/bnv/) (Xia et al., 2013). ROI colours reflect Schaefer et al.'s network assignments. In panel (a), the size of the ROIs is proportional to their associated absolute value BSR. Panel (b) shows the correlations between the behavioral variables and the brain scores in each condition (i.e., data type) in the HCP-Development sample. Panel (c) shows the same information in the HCP-Aging sample. Error bars are the 95% confidence intervals from the bootstrap procedure. Confidence intervals that do not include zero reflect robust correlations between the respective behavioral variable and the brain score in a given condition across all HCP-Development/Aging participants (as appropriate). In panels (b, c), significant brain-behavior correlations replicated across all the supplemental analyses (including analyses based on the Gordon atlas and analyses with no race-related covariates) are within red line rectangles. LV= latent variable. BSR = bootstrap ratio. GMV = gray matter volume. Task = inhibitory control (Go/No-Go) task. Schaefer networks: TP= temporo-parietal. SAL-VAN = salience/ventral attention. LB = limbic. DMN = default mode. DAN = dorsal attention. SM-*A* =somatomotor-A. SM-*B* =somatomotor-B. VIS = visual. (For interpretation of the references to colour in this figure legend, the reader is referred to the web version of this article.)

(task-related $BOLD_{SV}$, functional differentiation during task) in the HCP-Development sample. In the HCP-Aging sample, we examined mediation effects of task and resting state $BOLD_{sv}$ (PLS LV1, Fig. 4-c) via functional flexibility and task-related network differentiation (LV2, Fig. 5-d). The LV1 flexibility and dedifferentiation scores score were not included in the analyses because their associations with adversity were more difficult to accommodate within the model depicted in Fig. 1-c and they were not replicated across all supplemental analyses. Biological aging was not included in any of the mediation analyses due to its weak correlations with adversity and psychological resilience/risk in both samples (*r*s from 0.09 to 0.10).

3.2.1. HCP-Development

The results did not support our hypothesis that $BOLD_{SV}$ would explain the shared variance between adversity exposure and psychopathology risk through its functional network correlates (i.e., task-related network differentiation) (see Fig. 6-a and Table 2).

3.2.2. HCP-Aging

We only found evidence of resting state $BOLD_{SV}$ mediation effects via task-rest functional network flexibility (see Fig. 6-c and Table 2), but not via task-related functional network dedifferentiation (see Fig. 6-b and Table 2). The results presented in Fig. 6-c thus imply that widespread adversity-related reductions in resting state $BOLD_{SV}$ are associated with greater SM/Control, but reduced DMN/SAL-VAN functional flexibility, which are, in turn, linked to higher psychopathology risk. These results were replicated in the corresponding supplemental analyses (see Figure S7 and Table S10).

3.3. Gene expression profiles linked to adversity, resilience and AD risk

3.3.1. Gene expression profile linked to adversity exposure and resilience

A behavioral PLS analysis, based on the abagen-outputted ROI x gene expression matrix, identified a sole gene expression profile ($p = 10^{-}5$), which accounted for 83.81% in the brain-gene expression covariance. This gene LV was linked positively to the resilience, $r = 0.30$, 95% CI = [.24; 0.39] but negatively to the adversity-relevant, $r = -0.40$, 95% CI = [−0.50; −0.32] brain LV (see Fig. 7-b). Given the relationship between the resilience-associated brain patterns in the HCP-Development and HCP-Aging samples (see Fig. 5-c, d), the identified gene LV was positively linked to the HCP-Aging, but negatively linked to the HCP-Developmental neural senescence/maturation patterns.

3.3.2. GO enrichment patterns

The enrichment analysis (Fulcher et al., 2021) suggested that the HCP-Aging resilience brain profile was positively, whereas the HCP-Development was negatively, linked to greater expression of genes involved in positive regulation, as well as modulation, of postsynaptic inhibitory potential (both corrected *p*-values of 0.012, see Fig. 7-a; see Supplemental Materials for replication of these effects with the Gordon atlas). No significant associations were detected for the adversity-relevant brain LV.

3.3.3. Relevance of the AD risk genes to the HCP-Development vs HCP-Aging resilience brain

Given the positive correlation between the gene and the HCP-Aging resilient brain LV, resilience-linked AD risk in the HCP-Aging was defined based on the number of the *AD_low* genes with negative BSRs and *AD_high* genes with positive BSRs. Complementarily, based on the

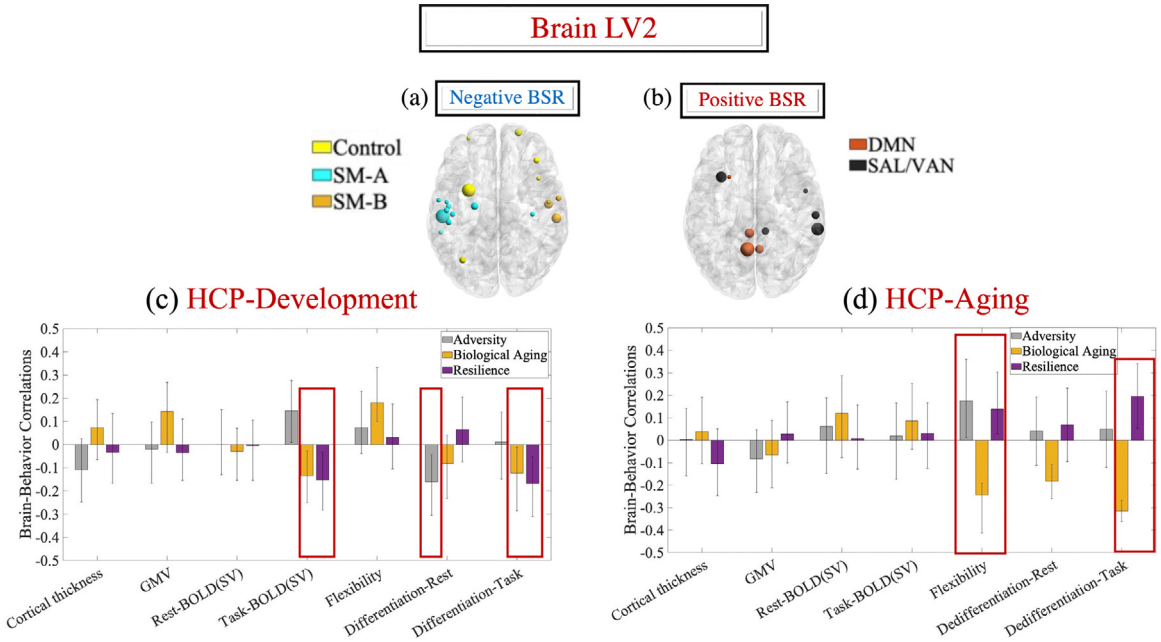

Fig. 5. Second extracted LV from the behavioral-PLS analysis linking adversity, resilience and biological aging to brain maturation (HCP-Development) or senescence (HCP-Aging). Panels (a) and (b) depict the Schaefer ROIs with robust loadings (absolute value BSR > 3) on the LV represented in panels (c) and (d). The ROIs were visualized with the BrainNet Viewer (http://www.nitrc.org/projects/bnv/) (Xia et al., 2013). ROI colours reflect Schaefer et al.'s network assignments. In panels (a) and (b), the size of the ROIs is proportional to their associated absolute value BSR. Panel (c) shows the correlations between the behavioral variables and the brain scores in each condition (i.e., data type) in the HCP-Development sample. Panel (d) shows the same information in the HCP-Aging sample. Error bars are the 95% confidence intervals from the bootstrap procedure. Confidence intervals that do not include zero reflect robust correlations between the respective behavioral variable and the brain score in a given condition across all HCP-Development/Aging participants (as appropriate). In panels (c) and (d), significant brain-behavior correlations replicated across all the supplemental analyses (including analyses based on the Gordon atlas and analyses with no race-related covariates) are within red line rectangles. LV= latent variable. BSR = bootstrap ratio. GMV = gray matter volume. Task = inhibitory control (Go/No-Go) task. Schaefer networks: DMN = default mode. SAL-VAN = salience/ventral attention. SM-*A* =somatomotor-A. SM-*B* =somatomotor-B. (For interpretation of the references to colour in this figure legend, the reader is referred to the web version of this article.)

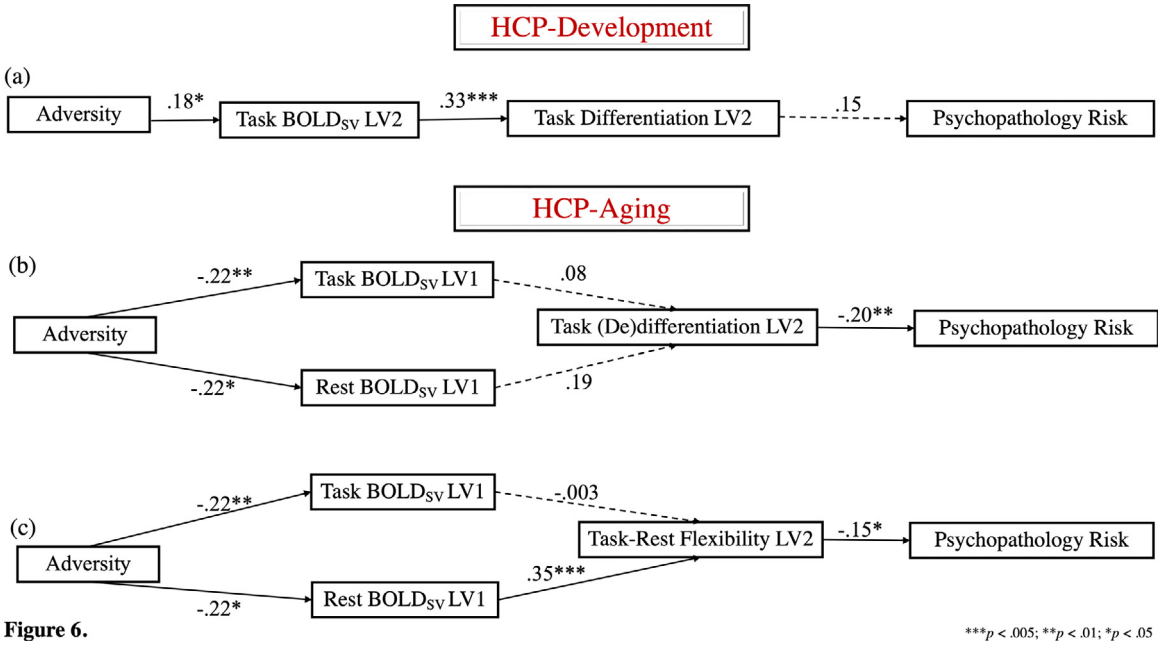

Figure 6.

***p < .005; **p < .01; *p < .05

Fig. 6. Mediational model linking adversity exposure to psychopathology risk in HCP-Development (a) and HCP-Aging (b,c). A dashed line indicates a statistically non-significant path ($p > .05$).

Table 2
Standardized Statistical Parameters for the Mediational Models Linking Adversity to Psychopathology Risk.

Mediator 1/Mediator 2	Effect of IV on Mediator 1 (*p*)	Unique Effect of Mediator 1 on Mediator 2 (*p*)	Unique Effect of Mediator 2 on DV (*p*)	Indirect Effect (*SE*)	95% CI Indirect Effect
HCP-Development					
Task $BOLD_{SV}$/Differentiation	.18 (0.019)	.33 (0.00001)	.15 (0.062)	.008 (0.006)	[−0.001;.023]
HCP-Aging					
Rest $BOLD_{SV}$/Task Differentiation[a]	−0.22 (0.012)	.19 (0.08)	−0.20 (0.007)	.008 (0.007)	[−0.001; 0.025]
Task $BOLD_{SV}$/Task Differentiation[a]	−0.22 (0.005)	.08 (0.40)	−0.20 (0.007)	.004 (0.005)	[−0.005; 0.016]
Rest $BOLD_{SV}$/Flexibility[b]	−0.22 (0.012)	.35 (0.0003)	−0.15 (0.039)	.012 (0.009)	[.0001; 0.034]
Task $BOLD_{SV}$/Flexibility[b]	−0.22 (0.005)	−0.003 (0.97)	−0.15 (0.039)	−0.0001 (0.003)	[−0.007; 0.007]

Note. *p* = statistical significance value. SE = bootstrap-based standard error. CI = confidence interval. [a]These paths are part of the same mediational model depicted in Fig. 6-b.[b]These paths are part of the same mediational model depicted in Fig. 6-c. IV = independent variable. DV = dependent variable.

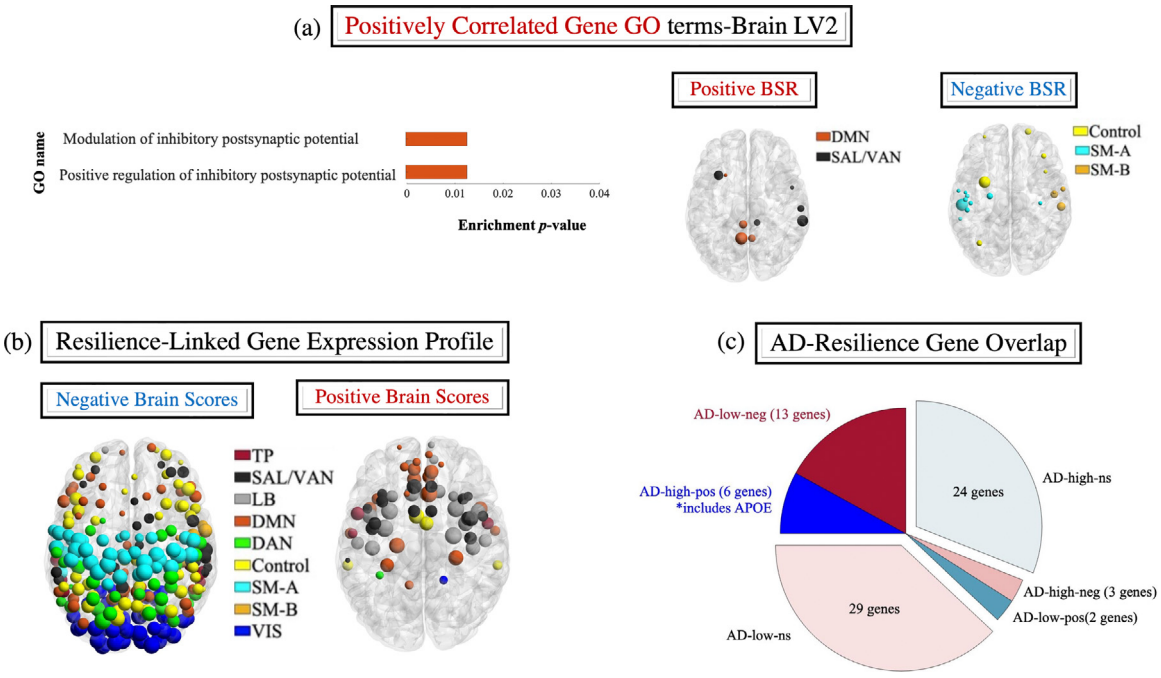

Fig. 7. Results of the transcriptomic and AD overlap analyses. Output of the enrichment analysis conducted with Fulcher et al. (2021) software toolbox on the accelerated brain development LV linked positively (HCP-Aging)/negatively (HCP-Development) to resilience (panel a). Panel (a) depicts only the ROIs with an absolute value BSR > 3 on the identified brain LV (see Fig. 5). Panel (b) represents the spatial expression map of the gene LV identified in behavioral PLS analysis 2. The ROIs were visualized with the BrainNet Viewer (http://www.nitrc.org/projects/bnv/) (Xia et al., 2013). ROI colours reflect Schaefer et al.'s network assignments and their size is proportional to how strongly they express the gene LV (i.e., the absolute value of the associated brain score). Panel (c) depicts the results of the AD-resilience gene LV overlap analyses. LV= latent variable. BSR = bootstrap ratio. Schaefer networks: TP= temporo-parietal. SAL-VAN = salience/ventral attention. LB = limbic. DMN = default mode. DAN = dorsal attention. SM-*A* =somatomotor-A. SM-*B* =somatomotor-B. VIS = visual.

negative correlation between the gene and HCP-Development resilient brain LV, resilience-linked AD risk in the HCP-Development was derived from the number of the *AD_high* genes with negative BSRs and *AD_low* genes with positive BSRs. There was no evidence of a significant association between the HCP-Development resilient brain profile and AD risk (permutation-based $p = .28$). We found though support for a significant association between the HCP-Aging resilient brain profile and AD risk (permutation-based $p = .0002$) (see Fig. 7-c).

4. Discussion

The substantial long-term damage inflicted by life adversities presumably stems, at least partly, from psychological mechanisms supporting initial adaptation, such as accelerated neurobiological aging (Belsky, 2019; Callaghan and Tottenham, 2016; McLaughlin et al., 2014, 2016). Using lifespan HCP data, our study replicates the association between recent adversity exposure and accelerated biological and functional brain development/aging. The latter is most salient in higher-order association systems (i.e., DMN, SAL-VAN, DAN, Control) which are known for their protracted developmental trajectories and enhanced lifespan vulnerability to psychiatric disorders (Cai et al., 2021; Dwyer et al., 2014; Ho et al., 2021; Kaiser et al., 2015; Sydnor et al., 2021). More importantly, our investigation extends this literature by identifying age-specific patterns of apparent acceleration/deceleration in brain development/senescence linked to resilience and earlier (adolescence) versus delayed (middle-age) biological aging. Suggestive of a partially antagonistic relationship between short-term resilience and longer term psychological adjustment (Colich et al., 2020), the neural aging correlates of middle-aged resilience were associated with transcriptomic markers of vulnerability to accelerated brain aging pathologies, specifically, AD.

4.1. Psychological resilience and brain development/aging

Paralleling previous proposals that the timing of adversity shapes its sequelae (Aschbacher et al., 2021; Gee and Casey, 2015; Nelson and Gabard-Durnam, 2020), we unveiled complementary neural signatures of psychological resilience in adolescence versus middle age. These profiles reflected the divergent developmental/aging patterns of SM/Control versus DMN/SAL-VAN ROIs (see Fig. 5-c, d). In adolescence, greater resilience was linked to relatively faster functional maturation of SM/Control systems, as reflected by patterns of task-related $BOLD_{SV}$ and network differentiation (see Fig. 5-c). Complementarily, the HCP-Aging resilience profile reflected the divergent relationship of brain-wide resting state $BOLD_{SV}$ decrements, related to adversity, with sensory and control versus attentional and internally oriented processing system differentiation and flexibility (see Fig. 6-c). As such, it mainly captured the antithetic segregation and functional efficiency patterns of SM/Control versus DMN/SAL-VAN which are predictive of reduced psychopathology (i.e., the link between higher resilience and greater DMN/ SAL-VAN dedifferentiation and task-rest reorganization, but greater SM/Control differentiation and reduced task-rest reorganization, see Fig. 5-d). Whether these findings reflect divergent aging trajectories underpinning resilience and/or indicate the chronically high levels of cognitive effort engaged by individuals who successfully cope with adversity is a question for future research (see Finc et al., 2020 for a link between reduced DMN segregation/differentiation and greater cognitive effort).

Of note, the joint contributions of SM, SAL-VAN and the core DMN subsystem, reportedly subserving self-related processes (Andrews-Hanna et al., 2007), to resilience concur with recent proposals linking self-regulatory success to (internal) self-in-(external) context representations (Koban et al., 2021). The involvement of SM and SAL-VAN is further consonant with their putative function as transdiagnostic hubs, since sensory and attentional deficits constitute key psychopathology symptoms (Kebets et al., 2019; McTeague et al., 2017).

It is worth pointing out that extant evidence suggests that coupled maturational changes in structure and function, particularly in higher-order association systems subserving cognitive control-relevant function, are cornerstone to successful development in adolescence (cf. Baum et al., 2020). However, in our study, greater psychological resilience in both adolescence and middle adulthood was associated only with differences in *functional* maturation/aging timing. This raises the question of whether structure-function developmental/aging uncoupling could be one of the mechanisms underpinning the partially antagonistic relationship between short-term resilience and long-term psychological adjustment.

4.2. Neurogenetic substrates of the resilience-AD vulnerability overlap

Extending prior investigations on the interplay between genetic and neural architecture in shaping evolutionary and lifespan developmental processes, our present study testifies to the relevance of a yoked connectomics-transcriptomics approach to characterizing potential mechanisms underpinning vulnerability to brain disorders (Arnatkevičiūtė et al., 2021; Changeux et al., 2021; Fornito et al., 2015, 2019). Specifically, complementing prior findings on the contribution of negative affectivity and mood pathology to AD onset, we report that the brain senescence patterns predictive of short-term resilience in middle adulthood are associated with a gene expression profile implicated in AD risk (Cole et al., 2021; Dafsari and Jessen, 2020; De Jager et al., 2021; Kunkle et al., 2019). The transcriptomic signature of the brain aging profile positively associated with the adult, but negatively associated with the adolescent, resilient brain LV (see Fig. 5-c, d) was enriched for genes implicated in synaptic inhibition. These results are thus in line with the putative role of altered GABA-ergic inhibition in the mood- and AD-linked cognitive deficits, as well as the relevance of inhibitory/excitatory balance to adolescent neural plasticity and neurodevelopmental disorders (Larsen and Luna, 2018; Prevot and Sibille, 2021; Tang et al., 2021; Zacharopoulos et al., 2021).

Our neurogenetic results are thus compatible with the interpretation that immediate adaptation mechanisms linked to neurobiological aging may unleash a cascade of cellular processes that heighten long-term psychiatric and neurodegenerative risk (Dafsari and Jessen, 2020; McLaughlin et al., 2014, 2016). This proposal echoes prior reports that cellular changes precede by decades the clinical phase of AD, thereby opening a window of opportunity for earlier identification and interventions targeting at-risk individuals (De Strooper and Karran, 2016). An alternative interpretation warranting further study is that our resilience-linked neurogenetic results reflect a case of antagonistic pleiotropy (cf. Provenzano and Deleidi, 2021). Specifically, individuals who are genetically predisposed towards accelerated brain aging and later development of AD (e.g., Gonneaud et al., 2021) may show greater psychological resilience earlier in life, potentially through a less differentiated processing of the external milieu. The viability of this proposal is worth probing in future studies targeting interactions between genetically and environmentally (i.e., acute and chronic adversity) triggered acceleration in neurobiological aging, as well as their role in predicting psychological resilience across multiple timescales.

4.3. Brain profiles linked to the timing of biological aging

Our investigation focused on two key hormonal transition stages, reflecting female reproductive maturation and senescence, respectively (Laube et al., 2020; Rehbein et al., 2021). Our decision was based on prior evidence on the role of ovarian hormones in psychological resilience, an effect likely explained through their GABA-ergic and oxytocin mediated downregulation of HPA axis activity following stress exposure (Engel et al., 2019; Joffe et al., 2020; Süss et al., 2021). Moreover, the susceptibility of ovarian hormones to adverse life events renders it likely that they could (partly) explain stress modulation of brain development/aging trajectories (Eck and Bangasser, 2020; Gordon et al., 2018).

Our analyses revealed complementary patterns of association between accelerated biological and brain aging in the two age groups. Specifically, in line with prior evidence on the immediately adaptive value of precocious neurobiological aging in adolescence (Belsky, 2019; Brieant et al., 2021; Callaghan and Tottenham, 2016), in the HCP-Development sample, we detected a positive association between earlier pubertal timing and the accelerated functional neurodevelopment pattern predictive of resilience. Conversely, accelerated biological aging was robustly inversely linked to the resilience functional brain senescence profile characterised during the inhibitory control task in HCP-Aging (i.e., overlapping neural substrates of greater resilience and delayed biological aging). This finding suggests that in later life quick recovery and/or active resistance to stressors may depend (in part) on preservation of sex hormone-mediated (down)regulation of HPA axis activity and dampened reactivity to the external milieu, potentially due to the accelerated aging of functional networks underpinning environmental vigilance (i.e., SAL-VAN [cf., Fig. 5-b, S2-b), CON [cf. Figure S4-b,6-b), Dosenbach et al., 2007; Sadaghiani and D'Esposito, 2015; Seeley et al., 2007; Sridharan et al., 2008).

In neither sample was biological aging timing robustly associated with the number of recent negative experiences. This implies that accelerated maturation/senescence may be solely related to chronic, rather than acute, forms of adversity (Tooley et al., 2021) and/or only certain dimensions of adversity (i.e., exposure to violence, Colich et al., 2020).

4.4. Limitations and future directions

Our present findings could be extended in several ways. First, multiwave longitudinal data could be used to account for heterogenous reproductive and neural developmental trajectories through growth curve

analysis methods (Becht and Mills, 2020). Second, recent studies underscore the protective role of the brain's functional architecture against adversity-linked cardiometabolic risks (Miller et al., 2018). While we controlled for cardiometabolic functioning as a means of accounting for prior adversity exposure, its potential link to brain and biological aging patterns underpinning shorter- versus longer-term resilience would warrant further study. Third, the impact of adversity on biological aging in childhood/adolescence varies with genetic susceptibility to earlier maturation (Sun et al., 2020), an effect that may be worth probing across the life course. Fourth, future investigations combining hormonal measures with self, parental (for adolescents) or physician indices of biological aging (i.e., pubertal timing/menopausal status, e.g., Herting et al., 2021) could determine the mechanisms through which psychological resilience, as demonstrated immediately after exposure to stressful life events, may dampen or accentuate longer-term vulnerability to psychiatric and/or neurodegenerative disorders. Fifth, direct lifespan comparisons of chronic versus acute exposure to adversity (cf. Gee and Casey, 2015) may elucidate their distinguishable effects on reproductive and brain system-specific maturation/senescence, thereby helping personalize interventions for vulnerable individuals (Brieant et al., 2021; Burstein et al., 2021; Goldstein et al., 2021; Herzberg et al., 2021; Tyborowska et al., 2018). While a dimensional approach to adversity, similar to the one we used to estimate longer-term stress exposure, is currently thought to better capture the individual variability in long-term neurodevelopmental outcomes (e.g., Ellis et al., 2022), indices of cumulative stress exposure should nonetheless be included to provide further insight into the determinants of resilience (e.g., Seery et al., 2010, Seery et al., 2013). These measures would ideally be collected within a prospective longitudinal design, since retrospective assessments are prone to recall biases (for a meta-analysis, see Baldwin et al., 2019). Such in-depth phenotyping may be difficult to implement in studies as large as the Lifespan HCPs. However, this provides a useful illustration of how the exploratory work that is afforded by large high-quality multimodal databases can be developed in more depth through smaller studies carrying targeted phenotyping on a question of interest. Sixth, use of cellular senescence measures (e.g., DNA methylation, Schumacher et al., 2021) would enable inclusion of gender diverse samples and more in-depth exploration of resilience-relevant neurogenetic mechanisms, including potential sex differences (for a review, see McEwen et al., 2015). For instance, cellular aging indices would allow inquiries into how pre-/perinatal stressors (e.g., malnutrition, maternal traumatic experiences/inflammation) can interact with the offspring's genetic profile to shape their lifespan development, including biological aging rate and, thus, potentially their resilience against later life adversity (Chan et al., 2019; Goldstein et al., 2021; Krontira et al., 2020; Mareckova et al., 2020; Ramo-Fernandez et al., 2021). Seventh, there is compelling evidence that personal characteristics, such as sense of purpose, sprituality, and social-affective enrichment in the form of warm parenting in childhood/adolescence and supportive close relationships later in life can alleviate the sequelae of prior adversity exposure (Bowes et al., 2010; Feder et al., 2009; Gee, 2021; Gunnar et al., 2019; Kiecolt-Glaser et al., 2020; Luby et al., 2020; Manvelian and Sbarra, 2020; Sbarra and Coan, 2018; Toumbelekis et al., 2021). As such, more in-depth investigation of the unique mechanisms through which distinct intra- and interpersonal factors may protect against the malign effects of stressful life experiences would be worth pursuing in the future.

4.5. Conclusions

In sum, we documented the distinguishable patterns of accelerated/decelerated neurodevelopment linked to resilience in adolescence and middle adulthood, as well as the potential psychological benefit of earlier reproductive maturation, but delayed reproductive senescence. Additionally, we provided suggestive evidence that the neural aging mechanisms underpinning short-term psychological resilience in middle adulthood could be linked to increased long-term risk for accelerated brain senescence pathologies, such as AD.

Data statement

The raw data are available at https://nda.nih.gov/ccf/lifespan-studies upon completion of the relevant data use agreements. The data used in this report came from the Lifespan Human Connectome Project-Annual Release 2.0.

Code availability

We used already existing code, as specified in the main text with links for free download.

Conflict of interest

The authors declare no competing interests.

Credit authorship contribution statement

Raluca Petrican: Conceptualization, Methodology, Formal analysis, Data curation, Visualization, Writing – original draft. **Alex Fornito:** Methodology, Software, Resources, Writing – review & editing. **Natalie Jones:** Investigation, Writing – review & editing.

Acknowledgments

Data used in the preparation of this article were obtained from the Lifespan human connectome project (HCP) (https://www.humanconnectome.org/study/hcp-lifespan-development; https://www.humanconnectome.org/study/hcp-lifespan-aging), held in the NIMH Data Archive (NDA). The Lifespan HCP research is supported by grants U01MH109589, U01MH109589-S1, U01AG052564, and U01AG052564-S1 and by the 14 NIH Institutes and Centers that support the NIH Blueprint for Neuroscience Research, by the McDonnell Center for Systems Neuroscience at Washington University, by the Office of the Provost at Washington

University, by the University of Minnesota Medical School, by the University of Massachusetts Medical School, and by the University of California Los Angeles Medical School. This manuscript reflects the views of the authors and may not reflect the opinions or views of the NIH or HCP consortium investigators. The authors would like to thank Valentina Escott-Price for helpful discussions during the earlier stages of this manuscript.

Supplementary materials

Supplementary material associated with this article can be found, in the online version, at doi:10.1016/j.neuroimage.2022.119209.

References

Abdellaoui, A., Verweij, K., 2021. Dissecting polygenic signals from genome-wide association studies on human behaviour. Nat. Human Behav. 5, 686–694.
Achenbach, T.M., 1991. Manual For the Youth Self-Report and 1991 Profile. University of Vermont, Department of Psychiatry, Burlington, VT.
Achenbach, T.M., 2009. The Achenbach System of Empirically Based Assessment (ASEBA): Development, Findings, Theory and Applications. University of Vermont Research Center for Children, Youth and Families, Burlington, VT.
Achenbach, T.M. (2013). DSM Guide for the ASEBA. Burlington, VT: University of Vermont, Research Center for Children, Youth, & Families.
Amstadter, A.B., Myers, J.M., Kendler, K.S., 2014. Psychiatric resilience: longitudinal twin study. British J. Psych. 205, 275–280.
Andrews-Hanna, J.R., Snyder, A.Z., Vincent, J.L., Lustig, C., Head, D., Raichle, M.E., Buckner, R.L., 2007. Disruption of large-scale brain systems in advanced aging. Neuron 56, 924–935.
Arnatkevičiūtė, A., Fulcher, B.D., Fornito, A., 2019. A practical guide to linking brain-wide gene expression and neuroimaging data. Neuroimage 189, 353–367.

Arnatkeviciute, A., Fulcher, B.D., Oldham, S., Tiego, J., Paquola, C., Gerring, Z., Aquino, K., Hawi, Z., Johnson, B., Ball, G., Klein, M., Deco, G., Franke, B., Bellgrove, M.A., Fornito, A., 2021. Genetic influences on hub connectivity of the human connectome. Nat. Commun. 12, 4237.

Aschbacher, K., Hagan, M., Steine, I.M., Rivera, L., Cole, S., Baccarella, A., Epel, E.S., Lieberman, A., Bush, N.R., 2021. Adversity in early life and pregnancy are immunologically distinct from total life adversity: macrophage-associated phenotypes in women exposed to interpersonal violence. Transl. Psychiatry 11, 391.

Baldwin, J.R., Reuben, A., Newbury, J.B., Danese, A., 2019. Agreement between prospective and retrospective measures of childhood maltreatment: a systematic review and meta-analysis. JAMA Psychiatry 76, 584–593.

Ball, G., Seidlitz, J., Beare, R., Seal, M.L., 2020. Cortical remodelling in childhood is associated with genes enriched for neurodevelopmental disorders. Neuroimage 215, 116803.

Baracchini, G., Mišić, B., Setton, R., Mwilambwe-Tshilobo, L., Girn, M., Nomi, J.S., Uddin, L.Q., Turner, G.R., Spreng, R.N., 2021. Inter-regional BOLD signal variability is an organizational feature of functional brain networks. Neuroimage, 118149 doi:10.1016/j.neuroimage.2021.118149, Advance online publication.

Bassett, D.S., Wymbs, N.F., Porter, M.A., Mucha, P.J., Carlson, J.M., Grafton, S.T., 2011. Dynamic reconfiguration of human brain networks during learning. Proc. Natl. Acad. Sci. U.S.A. 108, 7641–7646.

Becht, A.I., Mills, K.L., 2020. Modeling individual differences in brain development. Biol. Psychiatry 88, 63–69.

Belsky, J., 2019. Early-life adversity accelerates child and adolescent development. Curr. Dir. Psychol. Sci. 28, 241–246.

Beurel, E., Toups, M., Nemeroff, C.B., 2020. The bidirectional relationship of depression and inflammation: double trouble. Neuron 107, 234–256.

Bookheimer, S.Y., Salat, D.H., Terpstra, M., Ances, B.M., Barch, D.M., Buckner, R.L., Burgess, G.C., Curtiss, S.W., Diaz-Santos, M., Elam, J.S., Fischl, B., Greve, D.N., Hagy, H.A., Harms, M.P., Hatch, O.M., Hedden, T., Hodge, C., Japardi, K.C., Kuhn, T.P., Ly, T.K., … Yacoub, E., 2019. The lifespan human connectome project in aging: an overview. Neuroimage 185, 335–348.

Bowes, L., Maughan, B., Caspi, A., Moffitt, T.E., Arseneault, L., 2010. Families promote emotional and behavioural resilience to bullying: evidence of an environmental effect. J. Child Psychol. Psychiatry 51, 809–817.

Braveman, P.A., Cubbin, C., Egerter, S., Chideya, S., Marchi, K.S., Metzler, M., Posner, S., 2005. Socioeconomic status in health research: one size does not fit all. JAMA 294, 2879–2888.

Brieant, A.E., Sisk, L.M., Gee, D.G., 2021. Associations among negative life events, changes in cortico-limbic connectivity, and psychopathology in the ABCD Study. Dev. Cogn. Neurosci. 52, 101022.

Burstein, O., Simon, N., Simchon-Tenenbaum, Y., Rehavi, M., Franko, M., Shamir, A., Doron, R., 2021. Moderation of the transgenerational transference of antenatal stress-induced anxiety. Transl. Psychiatry 11, 268.

Cai, W., Ryali, S., Pasumarthy, R., Talasila, V., Menon, V., 2021. Dynamic causal brain circuits during working memory and their functional controllability. Nat. Commun. 12, 3314.

Callaghan, B.L., Tottenham, N., 2016. The Stress Acceleration Hypothesis: effects of early-life adversity on emotion circuits and behavior. Curr. Opin. Behav. Sci. 7, 76–81.

Cao, P., Chen, C., Liu, A., Shan, Q., Zhu, X., Jia, C., Peng, X., Zhang, M., Farzinpour, Z., Zhou, W., Wang, H., Zhou, J.N., Song, X., Wang, L., Tao, W., Zheng, C., Zhang, Y., Ding, Y.Q., Jin, Y., Xu, L., … Zhang, Z., 2021. Early-life inflammation promotes depressive symptoms in adolescence via microglial engulfment of dendritic spines. Neuron doi:10.1016/j.neuron.2021.06.012, S0896-6273(21)00427-X.

Chan, K.L., Lo, C., Ho, F.K., Leung, W.C., Yee, B.K., Ip, P., 2019. The association between intimate partner violence against women and newborn telomere length. Transl. Psychiatry 9, 239.

Chan, M., Park, D.C., Savalia, N.K., Petersen, S.E., Wig, G.S., 2014. Decreased segregation of brain systems across the healthy adult lifespan. Proc. Natl. Acad. Sci. U.S.A. 111, E4997–E5006.

Chan, M.Y., Na, J., Agres, P.F., Savalia, N.K., Park, D.C., Wig, G.S., 2018. Socioeconomic status moderates age-related differences in the brain's functional network organization and anatomy across the adult lifespan. Proc. Natl. Acad. Sci. U.S.A. 115, E5144–E5153.

Changeux, J.P., Goulas, A., Hilgetag, C.C., 2021. A connectomic hypothesis for the hominization of the brain. Cerebral Cortex 31, 2425–2449.

Cheng, W., Luo, N., Zhang, Y., Zhang, X., Tan, H., Zhang, D., Sui, J., Yue, W., Yan, H., 2021. DNA methylation and resting brain function mediate the association between childhood urbanicity and better speed of processing. Cerebral Cortex bhab117. doi:10.1093/cercor/bhab117, Advance online publication.

Cole, J.J., McColl, A., Shaw, R., Lynall, M.E., Cowen, P.J., de Boer, P., Drevets, W.C., Harrison, N., Pariante, C., Pointon, L., consortium, N.I.M.A., Goodyear, C., Bullmore, E., Cavanagh, J, 2021. No evidence for differential gene expression in major depressive disorder PBMCs, but robust evidence of elevated biological ageing. Transl. Psychiatry 11, 404.

Colich, N.L., Rosen, M.L., Williams, E.S., McLaughlin, K.A., 2020. Biological aging in childhood and adolescence following experiences of threat and deprivation: a systematic review and meta-analysis. Psychol. Bull. 146, 721–764.

Collishaw, S., Hammerton, G., Mahedy, L., Sellers, R., Owen, M.J., Craddock, N., Thapar, A.K., Harold, G.T., Rice, F., Thapar, A., 2016. Mental health resilience in the adolescent offspring of parents with depression: a prospective longitudinal study. Lancet Psych. 3, 49–57.

Cummings, E.M., Miller-Graff, L.E., 2015. Emotional security theory: an emerging theoretical model for youths' psychological and physiological responses across multiple developmental contexts. Curr. Dir. Psychol. Sci. 24, 208–213.

Dafsari, F.S., Jessen, F., 2020. Depression—an underrecognized target for prevention of dementia in Alzheimer's disease. Transl. Psychiatry 10, 160.

Dale, A.M., Fischl, B., Sereno, M.I., 1999. Cortical surface-based analysis. I. Segmentation and surface reconstruction. Neuroimage 9, 179–194.

Darrow, S.M., Verhoeven, J.E., Révész, D., Lindqvist, D., Penninx, B.W., Delucchi, K.L., Wolkowitz, O.M., Mathews, C.A., 2016. The Association Between Psychiatric Disorders and telomere length: a meta-analysis involving 14,827 persons. Psychosom. Med. 78, 776–787.

Davidow, J.Y., Sheridan, M.A., Van Dijk, K., Santillana, R.M., Snyder, J., Vidal Bustamante, C.M., Rosen, B.R., Somerville, L.H., 2019. Development of prefrontal cortical connectivity and the enduring effect of learned value on cognitive control. J. Cogn. Neurosci. 31, 64–77.

De Jager, C.H., White, C.C., Bennett, D.A., Ma, Y., 2021. Neuroticism alters the transcriptome of the frontal cortex to contribute to the cognitive decline and onset of Alzheimer's disease. Transl Psychiatry 11, 139.

De Strooper, B., Karran, E., 2016. The Cellular Phase of Alzheimer's Disease. Cell 164, 603–615.

Devanand, D.P., Kim, M.K., Paykina, N., Sackeim, H.A., 2002. Adverse life events in elderly patients with major depression or dysthymic disorder and in healthy-control subjects. Am. J. Ger. Psychiatry 10, 265–274.

Dosenbach, N.U., Fair, D.A., Miezin, F.M., Cohen, A.L., Wenger, K.K., Dosenbach, R.A., Fox, M.D., Snyder, A.Z., Vincent, J.L., Raichle, M.E., Schlaggar, B.L., Petersen, S.E., 2007. Distinct brain networks for adaptive and stable task control in humans. Proc. Natl. Acad. Sci. U.S.A. 104, 11073–11078.

Dwyer, D.B., Harrison, B.J., Yücel, M., Whittle, S., Zalesky, A., Pantelis, C., Allen, N.B., Fornito, A., 2014. Large-scale brain network dynamics supporting adolescent cognitive control. J. Neurosci. 34, 14096–14107.

Eck, S.R., Bangasser, D.A., 2020. The effects of early life stress on motivated behaviors: a role for gonadal hormones. Neurosci. Biobehav. Rev. 119, 86–100.

Ellis, B.J., Sheridan, M.A., Belsky, J., McLaughlin, K.A., 2022. Why and how does early adversity influence development? Toward an integrated model of dimensions of environmental experience. Dev. Psychopathol. 1–25. doi:10.1017/S0954579421001838, Advance online publication.

Engel, S., Klusmann, H., Ditzen, B., Knaevelsrud, C., Schumacher, S., 2019. Menstrual cycle-related fluctuations in oxytocin concentrations: a systematic review and meta–analysis. Front. Neuroendocrinol. 52, 144–155.

Fang, Y., Scott, L., Song, P., Burmeister, M., Sen, S., 2020. Genomic prediction of depression risk and resilience under stress. Nat. Human Behav. 4, 111–118.

Faust, T.E., Gunner, G., Schafer, D.P., 2021. Mechanisms governing activity-dependent synaptic pruning in the developing mammalian CNS. Nat. Rev. Neurosci. 22, 657–673.

Feder, A., Nestler, E.J., Charney, D.S., 2009. Psychobiology and molecular genetics of resilience. Nat. Rev. Neurosci. 10, 446–457.

Finc, K., Bonna, K., He, X., Lydon-Staley, D.M., Kühn, S., Duch, W., Bassett, D.S., 2020. Dynamic reconfiguration of functional brain networks during working memory training. Nat. Commun. 11, 2435.

Fischl, B., Liu, A., Dale, A.M., 2001. Automated manifold surgery: constructing geometrically accurate and topologically correct models of the human cerebral cortex. IEEE Transacti. Med. Imaging 20, 70–80.

Fischl, B., Salat, D.H., Busa, E., Albert, M., Dieterich, M., Haselgrove, C., van der Kouwe, A., Killiany, R., Kennedy, D., Klaveness, S., Montillo, A., Makris, N., Rosen, B., Dale, A.M., 2002. Whole brain segmentation: automated labeling of neuroanatomical structures in the human brain. Neuron 33, 341–355.

Fischl, B., Sereno, M.I., Dale, A.M., 1999a. Cortical surface-based analysis. II: inflation, flattening, and a surface-based coordinate system. Neuroimage 9, 195–207.

Fischl, B., Sereno, M.I., Tootell, R.B., Dale, A.M., 1999b. High-resolution intersubject averaging and a coordinate system for the cortical surface. Hum. Brain Mapp. 8, 272–284.

Fornito, A., Zalesky, A., Breakspear, M.J., 2015. The connectomics of brain disorders. Nat. Rev. Neurosci. 16, 159–172.

Fornito, A., Arnatkevicuite, A., Fulcher, B.D., 2019. Bridging the gap between the brain's transcriptome and connectome. Trends Cogn. Sci. (Regul. Ed.) 23, 34–50.

Fortier, C.B., Amick, M.M., Grande, L., McGlynn, S., Kenna, A., Morra, L., Clark, A., Milberg, W.P., McGlinchey, R.E., 2014. The Boston Assessment of Traumatic Brain Injury-Lifetime (BAT-L) semistructured interview: evidence of research utility and validity. J. Head Trauma Rehabil. 29, 89–98.

Fulcher, B.D., Little, M.A., Jones, N.S., 2013. Highly comparative time-series analysis: the empirical structure of time series and their methods. J. Royal Soci. Interface 10, 20130048.

Fulcher, B.D., Arnatkeviciute, A., Fornito, A., 2021. Overcoming false-positive gene-category enrichment in the analysis of spatially resolved transcriptomic brain atlas data. Nat. Commun. 12, 2669.

Gabard-Durnam, L.J., Gee, D.G., Goff, B., Flannery, J., Telzer, E., Humphreys, K.L., Lumian, D.S., Fareri, D.S., Caldera, C., Tottenham, N., 2016. Stimulus-elicited connectivity influences resting-state connectivity years later in human development: a prospective study. J. Neurosci. 36, 4771–4784.

Garrett, D.D., Skowron, A., Wiegert, S., Adolf, J., Dahle, C.L., Lindenberger, U., Raz, N., 2021. Lost dynamics and the dynamics of loss: longitudinal compression of brain signal variability is coupled with declines in functional integration and cognitive performance. Cerebral Cortex doi:10.1093/cercor/bhab154.

Garrett, D.D., Epp, S.M., Kleemeyer, M., Lindenberger, U., Polk, T.A., 2020. Higher performing older adults upregulate brain signal variability in response to feature-rich sensory input. Neuroimage 217, 116836.

Garrett, D.D., Kovacevic, N., McIntosh, A.R., Grady, C.L., 2013. The modulation of BOLD variability between cognitive states varies by age and processing speed. Cerebral Cortex 23, 684–693.

Gee, D.G., 2021. Early Adversity and Development: parsing Heterogeneity and Identifying Pathways of Risk and Resilience. Am. J. Psychiatry 178, 998–1013.

Gee, D.G., Casey, B.J., 2015. The impact of developmental timing for stress and recovery. Neurobiol. Stress 1, 184–194.

Gee, D.G., Gabard-Durnam, L.J., Flannery, J., Goff, B., Humphreys, K.L., Telzer, E.H., Hare, T.A., Bookheimer, S.Y., Tottenham, N., 2013. Early developmental emergence of human amygdala-prefrontal connectivity after maternal deprivation. Proc. Natl. Acad. Sci. U.S.A. 110, 15638–15643.

Geng, F., Botdorf, M., Riggins, T., 2021. How behavior shapes the brain and the brain shapes behavior: insights from memory development. Journal of Neurosci. 41, 981–990.

Giedd, J.N., Blumenthal, J., Jeffries, N.O., Castellanos, F.X., Liu, H., Zijdenbos, A., Paus, T., Evans, A.C., Rapoport, J.L., 1999. Brain development during childhood and adolescence: a longitudinal MRI study. Nat. Neurosci. 2, 861–863.

Glasser, M.F., Sotiropoulos, S.N., Wilson, J.A., Coalson, T.S., Fischl, B., Andersson, J.L., Xu, J., Jbabdi, S., Webster, M., Polimeni, J.R., Van Essen, D.C., Jenkinson, M., Consortium, WU-Minn HCP, 2013. The minimal preprocessing pipelines for the human connectome project. Neuroimage 80, 105–124.

Goldstein, J.M., Cohen, J.E., Mareckova, K., Holsen, L., Whitfield-Gabrieli, S., Gilman, S.E., Buka, S.L., Hornig, M., 2021. Impact of prenatal maternal cytokine exposure on sex differences in brain circuitry regulating stress in offspring 45 years later. Proc. Natl. Acad. Sci. U.S.A. 118, e2014464118.

Gonneaud, J., Baria, A.T., Pichet Binette, A., Gordon, B.A., Chhatwal, J.P., Cruchaga, C., Jucker, M., Levin, J., Salloway, S., Farlow, M., Gauthier, S., Benzinger, T., Morris, J.C., Bateman, R.J., Breitner, J., Poirier, J., Vachon-Presseau, E., Villeneuve, S.Alzheimer's Disease Neuroimaging Initiative (ADNI), Dominantly Inherited Alzheimer Network (DIAN) Study Group, … Pre-symptomatic Evaluation of Experimental or Novel Treatments for Alzheimer's Disease (PREVENT-AD) Research Group, 2021. Accelerated functional brain aging in pre-clinical familial Alzheimer's disease. Nat. Commun. 12, 5346.

Gordon, E.M., Laumann, T.O., Adeyemo, B., Huckins, J.F., Kelley, W.M., Petersen, S.E., 2016. Generation and evaluation of a cortical area parcellation from resting-state correlations. Cerebral Cortex 26, 288–303.

Gordon, J.L., Rubinow, D.R., Eisenlohr-Moul, T.A., Xia, K., Schmidt, P.J., Girdler, S.S., 2018. Efficacy of transdermal estradiol and micronized progesterone in the prevention of depressive symptoms in the menopause transition: a randomized clinical trial. JAMA Psychiatry 75, 149–157.

Grady, C.L., Garrett, D.D., 2018. Brain signal variability is modulated as a function of internal and external demand in younger and older adults. Neuroimage 169, 510–523.

Grahek, I., Shenhav, A., Musslick, S., Krebs, R.M., Koster, E.H., 2019. Motivation and cognitive control in depression. Neurosci. Biobehav. Rev. 102, 371–381.

Grayson, D.S., Fair, D.A., 2017. Development of large-scale functional networks from birth to adulthood: A guide to the neuroimaging literature. NeuroImage 160, 15–31.

Griffanti, L., Salimi-Khorshidi, G., Beckmann, C.F., Auerbach, E.J., Douaud, G., Sexton, C.E., Zsoldos, E., Ebmeier, K.P., Filippini, N., Mackay, C.E., Moeller, S., Xu, J., Yacoub, E., Baselli, G., Ugurbil, K., Miller, K.L., Smith, S.M., 2014. ICA-based artefact removal and accelerated fMRI acquisition for improved resting state network imaging. Neuroimage 95, 232–247.

Guerrero, A., De Strooper, B., Arancibia-Cárcamo, I.L., 2021. Cellular senescence at the crossroads of inflammation and Alzheimer's disease. Trends Neurosci. doi:10.1016/j.tins.2021.06.007, S0166-2236(21)00119-3Advance online publication.

Gunnar, M.R., DePasquale, C.E., Reid, B.M., Donzella, B., Miller, B.S., 2019. In: Pubertal Stress Recalibration Reverses the Effects of Early Life Stress in Postinstitutionalized Children, 116. Proceedings of the National Academy of Sciences of the United States of America, pp. 23984–23988.

Hair, J.F., Black, W.C., Babin, B.J., Anderson, R.E., Tatham, R.L., 2014. Multivariate Data Analysis. Pearson Education Limited.

Han, L., Schnack, H.G., Brouwer, R.M., Veltman, D.J., van der Wee, N., van Tol, M.J., Aghajani, M., Penninx, B., 2021. Contributing factors to advanced brain aging in depression and anxiety disorders. Transl Psychiatry 11, 402.

Hansen, J.Y., Markello, R.D., Vogel, J.W., Seidlitz, J., Bzdok, D., Misic, B., 2021. Mapping gene transcription and neurocognition across human neocortex. Nat. Human Behav. doi:10.1038/s41562-021-01082-z.

Harerimana, N.V., Liu, Y., Gerasimov, E.S., Duong, D., Beach, T.G., Reiman, E.M., et al., 2022. Genetic evidence supporting a causal role of depression on Alzheimer's disease. Biol. Psychiatry doi:10.1016/j.biopsych.2021.11.025.

Harms, M.P., Somerville, L.H., Ances, B.M., Andersson, J., Barch, D.M., Bastiani, M., Bookheimer, S.Y., Brown, T.B., Buckner, R.L., Burgess, G.C., Coalson, T.S., Chappell, M.A., Dapretto, M., Douaud, G., Fischl, B., Glasser, M.F., Greve, D.N., Hodge, C., Jamison, K.W., Jbabdi, S., … Yacoub, E., 2018. Extending the human connectome project across ages: imaging protocols for the lifespan development and aging projects. Neuroimage 183, 972–984.

Harold, G.T., Sellers, R., 2018. Annual research review: interparental conflict and youth psychopathology: an evidence review and practice focused update. J. Child Psychol. Psychiatry 59, 374–402.

Hawrylycz, M., Miller, J.A., Menon, V., Feng, D., Dolbeare, T., Guillozet-Bongaarts, A.L., … Lein, E., 2015. Canonical genetic signatures of the adult human brain. Nat. Neurosci. 18, 1832.

Hayes, A., Cai, L., 2007. Using heteroskedasticity-consistent standard error estimators in OLS regression: an introduction and software implementation. Behav. Res. Methods 39, 709–722.

Hayes, A.F., Scharkow, M., 2013. The relative trustworthiness of inferential tests of the indirect effect in statistical mediation analysis: does method really matter? Psychol. Sci. 10, 1918–1927.

Hayes, A.F., 2018. Introduction to Mediation, Moderation, and Conditional Process Analysis: A Regression-Based Approach, 2nd Edition Guilford Press, New York.

Heinzel, S., Lorenz, R.C., Brockhaus, W.R., Wüstenberg, T., Kathmann, N., Heinz, A., Rapp, M.A., 2014. Working memory load-dependent brain response predicts behavioral training gains in older adults. J. Neurosci. 34, 1224–1233.

Herting, M.M., Gautam, P., Spielberg, J.M., Kan, E., Dahl, R.E., Sowell, E.R., 2014. The role of testosterone and estradiol in brain volume changes across adolescence: a longitudinal structural MRI study. Hum. Brain Mapp. 35, 5633–5645.

Herting, M.M., Uban, K.A., Gonzalez, M.R., Baker, F.C., Kan, E.C., Thompson, W.K., Granger, D.A., Albaugh, M.D., Anokhin, A.P., Bagot, K.S., Banich, M.T., Barch, D.M., Baskin-Sommers, A., Breslin, F.J., Casey, B.J., Chaarani, B., Chang, L., Clark, D.B., Cloak, C.C., Constable, R.T., … Sowell, E.R., 2021. Correspondence between perceived pubertal development and hormone levels in 9-10 year-olds from the adolescent brain cognitive development study. Front Endocrinol. (Lausanne) 11, 549928.

Herzberg, M.P., McKenzie, K.J., Hodel, A.S., Hunt, R.H., Mueller, B.A., Gunnar, M.R., Thomas, K.M., 2021. Accelerated maturation in functional connectivity following early life stress: circuit specific or broadly distributed? Dev. Cogn. Neurosci. 48, 100922.

Ho, T.C., Walker, J.C., Teresi, G.I., Kulla, A., Kirshenbaum, J.S., Gifuni, A.J., Singh, M.K., Gotlib, I.H., 2021. Default mode and salience network alterations in suicidal and non–suicidal self-injurious thoughts and behaviors in adolescents with depression. Transl. Psychiatry 11, 38.

Hughes, C., Faskowitz, J., Cassidy, B.S., Sporns, O., Krendl, A.C., 2020. Aging relates to a disproportionately weaker functional architecture of brain networks during rest and task states. Neuroimage 209, 116521.

Ioannidis, K., Askelund, A.D., Kievit, R.A., van Harmelen, A.L., 2020. The complex neurobiology of resilient functioning after childhood maltreatment. BMC Med. 18, 32.

Jin, W.N., Shi, K., He, W., Sun, J.H., Van Kaer, L., Shi, F.D., Liu, Q., 2021. Neuroblast senescence in the aged brain augments natural killer cell cytotoxicity leading to impaired neurogenesis and cognition. Nat. Neurosci. 24, 61–73.

Joffe, H., de Wit, A., Coborn, J., Crawford, S., Freeman, M., Wiley, A., Athappilly, G., Kim, S., Sullivan, K.A., Cohen, L.S., Hall, J.E., 2020. Impact of estradiol variability and progesterone on mood in perimenopausal women with depressive symptoms. J. Clin. Endocrinol. Metab. 105, e642–e650.

Kaiser, R.H., Andrews-Hanna, J.R., Wager, T.D., Pizzagalli, D.A., 2015. Large-scale network dysfunction in major depressive disorder: a meta-analysis of resting-state functional connectivity. JAMA Psychiatry 72, 603–611.

Kalisch, R., Cramer, A., Binder, H., Fritz, J., Leertouwer, I., Lunansky, G., Meyer, B., Timmer, J., Veer, I.M., van Harmelen, A.L., 2019. Deconstructing and reconstructing resilience: a dynamic network approach. Perspect. Psycholog. Sci. 14, 765–777.

Kalisch, R., Baker, D.G., Basten, U., Boks, M.P., Bonanno, G.A., Brummelman, E., Chmitorz, A., Fernàndez, G., Fiebach, C.J., Galatzer-Levy, I., Geuze, E., Groppa, S., Helmreich, I., Hendler, T., Hermans, E.J., Jovanovic, T., Kubiak, T., Lieb, K., Lutz, B., Müller, M.B., … Kleim, B., 2017. The resilience framework as a strategy to combat stress-related disorders. Nat. Human Behavi. 1, 784–790.

Kebets, V., Holmes, A.J., Orban, C., Tang, S., Li, J., Sun, N., Kong, R., Poldrack, R.A., Yeo, B., 2019. Somatosensory-motor dysconnectivity spans multiple transdiagnostic dimensions of psychopathology. Biol. Psychiatry 86, 779–791.

Kendler, K.S., Lönn, S.L., Salvatore, J., Sundquist, J., Sundquist, K., 2017. Divorce and the onset of alcohol use disorder: a swedish population-based longitudinal cohort and co-relative study. Am. J. Psychiatry 174, 451–458.

Kiecolt-Glaser, J.K., Renna, M.E., Shrout, M.R., Madison, A.A., 2020. Stress reactivity: what pushes us higher, faster, and longer - and why it matters. Curr. Dir. Psychol. Sci. 29, 492–498.

Kim, G.W., Park, K., Jeong, G.W., 2018. Effects of sex hormones and age on brain volume in post-menopausal women. J Sex Med 15, 662–670.

Koban, L., Gianaros, P.J., Kober, H., Wager, T.D., 2021. The self in context: brain systems linking mental and physical health. Nat. Rev. Neurosci. 22, 309–322.

Krontira, A.C., Cruceanu, C., Binder, E.B., 2020. Glucocorticoids as mediators of adverse outcomes of prenatal stress. Trends Neurosci. 43, 394–405.

Kunkle, B.W., Grenier-Boley, B., Sims, R., Bis, J.C., Damotte, V., Naj, A.C., Boland, A., Vronskaya, M., van der Lee, S.J., Amlie-Wolf, A., Bellenguez, C., Frizatti, A., Chouraki, V., Martin, E.R., Sleegers, K., Badarinarayan, N., Jakobsdottir, J., Hamilton-Nelson, K.L., Moreno-Grau, S., … Olaso, R.Genetic and Environmental Risk in AD/Defining Genetic, Polygenic and Environmental Risk for Alzheimer's Disease Consortium (GERAD/PERADES), 2019. Genetic meta-analysis of diagnosed Alzheimer's disease identifies new risk loci and implicates Aβ, tau, immunity and lipid processing. Nat. Genet. 5, 414–430.

Larsen, B., Luna, B., 2018. Adolescence as a neurobiological critical period for the development of higher-order cognition. Neurosci. Biobehav. Rev. 94, 179–195.

Laube, C., van den Bos, W., Fandakova, Y., 2020. The relationship between pubertal hormones and experience-dependent plasticity: implications for cognitive training in adolescence. Dev. Cogn. Neurosci. 42, 100753.

Lindenberger, U., Lövdén, M., 2019. Brain plasticity in human lifespan development: the exploration–selection–refinement model. Ann. Rev. Develop. Psychol. 1, 197–222.

Liu, M., Backer, R.A., Amey, R.C., Splan, E.E., Magerman, A., Forbes, C.E., 2021. Context matters: situational stress impedes functional reorganization of intrinsic brain connectivity during problem-solving. Cerebral Cortex 31, 2111–2124.

Luby, J.L., Baram, T.Z., Rogers, C.E., Barch, D.M., 2020. Neurodevelopmental optimization after early-life adversity: cross-species studies to elucidate sensitive periods and brain mechanisms to inform early intervention. Trends Neurosci. 43, 744–751.

Lutz, M.W., Luo, S., Williamson, D.E., Chiba-Falek, O., 2020. Shared genetic etiology underlying late-onset Alzheimer's disease and posttraumatic stress syndrome. Alzheimer's Dementia 16, 1280–1292.

Ly, M., Karim, H.T., Becker, J.T., Lopez, O.L., Anderson, S.J., Aizenstein, H.J., Reynolds, C.F., Zmuda, M.D., Butters, M.A., 2021. Late-life depression and increased risk of dementia: a longitudinal cohort study. Transl. Psychiatry 11, 147.

Manvelian, A., Sbarra, D.A., 2020. Marital status, close relationships, and all-cause mortality: results from a 10-year study of nationally representative older adults. Psychosom. Med. 82, 384–392.

Mareckova, K., Marecek, R., Andryskova, L., Brazdil, M., Nikolova, Y.S., 2020. Maternal depressive symptoms during pregnancy and brain age in young adult offspring: findings from a prenatal birth cohort. Cerebral Cortex 30, 3991–3999.
McEwen, B.S., Gray, J., Nasca, C., 2015. Recognizing resilience: learning from the effects of stress on the brain. Neurobiol. Stress 1, 1–11.
McLaughlin, K.A., Sheridan, M.A., 2016. Beyond Cumulative Risk: A Dimensional Approach to Childhood Adversity. Current Directions in Psychological Science 25, 239–245.
McLaughlin, K. A., Sheridan, M. A., Lambert, H. K., 2014. Childhood adversity and neural development: deprivation and threat as distinct dimensions of early experience. Neuroscience and Biobehavioral Reviews 47, 578–591.
McLaughlin, K.A., Colich, N.L., Rodman, A.M., Weissman, D.G., 2020. Mechanisms linking childhood trauma exposure and psychopathology: a transdiagnostic model of risk and resilience. BMC Med. 18, 96.
McLaughlin, K.A., Sheridan, M.A., Humphreys, K.L., Belsky, J., Ellis, B.J., 2021. The value of dimensional models of early experience: thinking clearly about concepts and categories. Perspect. Psychol. Sci. 16, 1463–1472.
McTeague, L.M., Huemer, J., Carreon, D.M., Jiang, Y., Eickhoff, S.B., Etkin, A., 2017. Identification of common neural circuit disruptions in cognitive control across psychiatric disorders. Am. J. Psychiatry 174, 676–685.
Milan, L., Whittaker, J., 1995. Application of the parametric bootstrap to models that incorporation a singular value decomposition. J. Royal Statist. Soci., Series C (Applied Statistics) 44, 31–49.
Millar, P.R., Petersen, S.E., Ances, B.M., Gordon, B.A., Benzinger, T., Morris, J.C., Balota, D.A., 2020a. Evaluating the sensitivity of resting-state BOLD variability to age and cognition after controlling for motion and cardiovascular influences: a network-based approach. Cerebral Cortex 30, 5686–5701.
Millar, P.R., Ances, B.M., Gordon, B.A., Benzinger, T., Fagan, A.M., Morris, J.C., Balota, D.A., 2020b. Evaluating resting-state BOLD variability in relation to biomarkers of preclinical Alzheimer's disease. Neurobiol. Aging 96, 233–245.
Miller, G.E., Chen, E., Armstrong, C.C., Carroll, A.L., Ozturk, S., Rydland, K.J., Brody, G.H., Parrish, T.B., Nusslock, R., 2018. Functional connectivity in central executive network protects youth against cardiometabolic risks linked with neighborhood violence. Proc. Natl. Acad. Sci. U.S.A. 115, 12063–12068.
Miller, J.G., Ho, T.C., Humphreys, K.L., King, L.S., Foland-Ross, L.C., Colich, N.L., Ordaz, S.J., Lin, J., Gotlib, I.H., 2020. Early life stress, frontoamygdala connectivity, and biological aging in adolescence: a longitudinal investigation. Cerebral Cortex 30, 4269–4280.
Murtha, K., Larsen, B., Pines, A., Parkes, L., Moore, T.M., Adebimpe, A., Bertolero, M., Alexander-Bloch, A., Calkins, M.E., Davila, D.G., Lindquist, M.A., Mackey, A.P., Roalf, D.R., Scott, J.C., Wolf, D.H., Gur, R.C., Gur, R.E., Barzilay, R., Satterthwaite, T.D., 2022. Associations between neighborhood socioeconomic status, parental education, and executive system activation in youth. Cerebral Cortex bhac120. doi:10.1093/cercor/bhac120, Advance online publication.
Murthy, S., Gould, E., 2020. How early life adversity influences defensive circuitry. Trends Neurosci. 43, 200–212.
Nadig, A., Seidlitz, J., McDermott, C.L., Liu, S., Bethlehem, R., Moore, T.M., Mallard, T.T., Clasen, L.S., Blumenthal, J.D., Lalonde, F., Gur, R.C., Gur, R.E., Bullmore, E.T., Satterthwaite, T.D., Raznahan, A., 2021. Morphological integration of the human brain across adolescence and adulthood. Proc. Natl. Acad. Sci. U.S.A. 118, e2023860118.
Nelson 3rd, C.A., Gabard-Durnam, L.J., 2020. Early Adversity and Critical Periods: neurodevelopmental consequences of violating the expectable environment. Trends Neurosci. 43, 133–143.
Neubauer, A.C., Fink, A., 2009. Intelligence and neural efficiency. Neurosci. Biobehav. Rev. 33, 1004–1023.
Nievergelt, C.M., Maihofer, A.X., Klengel, T., Atkinson, E.G., Chen, C.Y., Choi, K.W., Coleman, J., Dalvie, S., Duncan, L.E., Gelernter, J., Levey, D.F., Logue, M.W., Polimanti, R., Provost, A.C., Ratanatharathorn, A., Stein, M.B., Torres, K., Aiello, A.E., Almli, L.M., Amstadter, A.B., … Koenen, K.C., 2019. International meta-analysis of PTSD genome-wide association studies identifies sex- and ancestry-specific genetic risk loci. Nat. Commun. 10, 4558.
Nomi, J.S., Bolt, T.S., Ezie, C., Uddin, L.Q., Heller, A.S., 2017. Moment-to-moment BOLD signal variability reflects regional changes in neural flexibility across the lifespan. J. Neurosci. 37, 5539–5548.
Oh, D.L., Jerman, P., Silvério Marques, S., Koita, K., Purewal Boparai, S.K., Burke Harris, N., Bucci, M, 2018. Systematic review of pediatric health outcomes associated with childhood adversity. BMC Pediatr. 18, 83.
Petersen, A.C., Crockett, L., Richards, M., Boxer, A., 1988. A self-report measure of pubertal status: reliability, validity, and initial norms. J. Youth Adolesc. 17, 117–133.
Petrican, R., Miles, S., Rudd, L., Wasiewska, W., Graham, K.S., Lawrence, A.D., 2021. Pubertal timing and functional neurodevelopmental alterations independently mediate the effect of family conflict on adolescent psychopathology. Dev. Cogn. Neurosci. 52, 101032.
Pezzulo, G., Zorzi, M., Corbetta, M., 2021. The secret life of predictive brains: what's spontaneous activity for? Trends Cogn. Sci. (Regul. Ed.) doi:10.1016/j.tics.2021.05.007, S1364-6613(21)00128-5.
Piekarski, D.J., Boivin, J.R., Wilbrecht, L., 2017. Ovarian hormones organize the maturation of inhibitory neurotransmission in the frontal cortex at puberty onset in female mice. Current Biol. 27, 1735–1745.
Power, J.D., Schlaggar, B.L., Petersen, S.E., 2015. Recent progress and outstanding issues in motion correction in resting state fMRI. Neuroimage 105, 536–551.
Prévot, T., Sibille, E., 2021. Altered GABA-mediated information processing and cognitive dysfunctions in depression and other brain disorders. Mol. Psychiatry 26, 151–167.
Provenzano, F., Deleidi, M., 2021. Reassessing neurodegenerative disease: immune protection pathways and antagonistic pleiotropy. Trends Neurosci. S0166-2236(21)00118-1.
Pur, D.R., Eagleson, R.A., de Ribaupierre, A., Mella, N., de Ribaupierre, S., 2019. Moderating effect of cortical thickness on BOLD signal variability age-related changes. Front Aging Neurosci. 11, 46.
Quackenbush, J., 2002. Microarray data normalization and transformation. Nat. Genet. 32, 496–501.
Ramirez, J.S.B., Graham, A.M., Thompson, J.R., Zhu, J.Y., Sturgeon, D., Bagley, J.L., Thomas, E., Papadakis, S., Perrone, A., Earl, E., Miranda Dominguez, O., Feczko, E., Fombone, E.J., Amaral, D.G., Nigg, J.T., Sullivan, E.L., Fair, D., 2020. Maternal interleukin-6 is associated with macaque offspring amygdala development and behavior. Cerebral Cortex 30, 1573–1585.
Ramo-Fernández, L., Gumpp, A.M., Boeck, C., Krause, S., Bach, A.M., Waller, C., Kolassa, I.T., Karabatsiakis, A., 2021. Associations between childhood maltreatment and DNA methylation of the oxytocin receptor gene in immune cells of mother-newborn dyads. Transl. Psychiatry 11, 449.
Rasmussen, J.M., Graham, A.M., Entringer, S., Gilmore, J.H., Styner, M., Fair, D.A., Wadhwa, P.D., Buss, C., 2019. Maternal Interleukin-6 concentration during pregnancy is associated with variation in frontolimbic white matter and cognitive development in early life. Neuroimage 185, 825–835.
Rehbein, E., Hornung, J., Poromaa, I.S., Derntl, B., 2021. Shaping of the female human brain by sex hormones: a review. Neuroendocrinology 111, 183–206.
Richards, M., Hardy, R., Wadsworth, M., 1997. The effects of divorce and separation on mental health in a national UK birth cohort. Psychol. Med. 27, 1121–1128.
Rickard, I.J., Frankenhuis, W.E., Nettle, D., 2014. Why are childhood family factors associated with timing of maturation? A role for internal prediction. Perspect. Psycholog. Sci. 9, 3–15.
Riddle, M., Potter, G.G., McQuoid, D.R., Steffens, D.C., Beyer, J.L., Taylor, W.D., 2017. Longitudinal cognitive outcomes of clinical phenotypes of late-life depression. Am. J. Geriatric Psychiatry 25, 1123–1134.
Robinson, E.C., Garcia, K., Glasser, M.F., Chen, Z., Coalson, T.S., Makropoulos, A., Bozek, J., Wright, R., Schuh, A., Webster, M., Hutter, J., Price, A., Cordero Grande, L., Hughes, E., Tusor, N., Bayly, P.V., Van Essen, D.C., Smith, S.M., Edwards, A.D., Hajnal, J., … Rueckert, D., 2018. Multimodal surface matching with higher-order smoothness constraints. Neuroimage 167, 453–465.
Roe, J.M., Vidal-Piñeiro, D., Sørensen, Ø., Brandmaier, A.M., Düzel, S., Gonzalez, H.A., Kievit, R.A., Knights, E., Kühn, S., Lindenberger, U., Mowinckel, A.M., Nyberg, L., Park, D.C., Pudas, S., Rundle, M.M., Walhovd, K.B., Fjell, A.M., Westerhausen, R.Australian Imaging Biomarkers and Lifestyle Flagship Study of Ageing, 2021. Asymmetric thinning of the cerebral cortex across the adult lifespan is accelerated in Alzheimer's disease. Nat. Commun. 12, 721.
Romeo, R.D., 2018. The metamorphosis of adolescent hormonal stress reactivity: a focus on animal models. Front. Neuroendocrinol. 49, 43–51.
Romeo, R.D., 2010. Adolescence: a central event in shaping stress reactivity. Dev. Psychobiol. 52, 244–253.
Rutter, M., 2013. Annual research review: resilience–clinical implications. J. Child Psychol. Psychiatry 54, 474–487.
Sadaghiani, S., D'Esposito, M, 2015. Functional characterization of the cingulo-opercular network in the maintenance of tonic alertness. Cerebral Cortex 25, 2763–2773.
Saikumar, J., Bonini, N.M., 2021. Synergistic effects of brain injury and aging: common mechanisms of proteostatic dysfunction. Trends Neurosci. doi:10.1016/j.tins.2021.06.003, S0166-2236(21)00115-6. Advance online publication.
Sbarra, D.A., Coan, J.A., 2018. Relationships and health: the critical role of affective science. Emotion Rev. 10, 40–54.
Schaefer, A., Kong, R., Gordon, E.M., Laumann, T.O., Zuo, X.N., Holmes, A.J., Eickhoff, S.B., Yeo, B., 2018. Local-global parcellation of the human cerebral cortex from intrinsic functional connectivity MRI. Cerebral Cortex 28, 3095–3114.
Schultz, D.H., Cole, M.W., 2016. Higher Intelligence is associated with less task-related brain network reconfiguration. J. Neurosci. 36, 8551–8561.
Schumacher, B., Pothof, J., Vijg, J., Hoeijmakers, J., 2021. The central role of DNA damage in the ageing process. Nature 592, 695–703.
Seeley, W.W., Menon, V., Schatzberg, A.F., Keller, J., Glover, G.H., Kenna, H., Reiss, A.L., Greicius, M.D., 2007. Dissociable intrinsic connectivity networks for salience processing and executive control. J. Neurosci. 27, 2349–2356.
Seery, M.D., Leo, R.J., Lupien, S.P., Kondrak, C.L., Almonte, J.L., 2013. An upside to adversity?: moderate cumulative lifetime adversity is associated with resilient responses in the face of controlled stressors. Psychol. Sci. 24, 1181–1189.
Seery, M.D., Holman, E.A., Silver, R.C., 2010. Whatever does not kill us: cumulative lifetime adversity, vulnerability, and resilience. J. Pers. Soc. Psychol. 99, 1025–1041.
Sele, S., Liem, F., Mérillat, S., Jäncke, L., 2021. Age-related decline in the brain: a longitudinal study on inter-individual variability of cortical thickness, area, volume, and cognition. Neuroimage 240, 118370. doi:10.1016/j.neuroimage.2021.118370, Advance online publication.
Selous, C., Kelly-Irving, M., Maughan, B., Eyre, O., Rice, F., Collishaw, S., 2020. Adverse childhood experiences and adult mood problems: evidence from a five-decade prospective birth cohort. Psychol. Med. 50, 2444–2451.
Sheng, J., Zhang, L., Feng, J., Liu, J., Li, A., Chen, W., Shen, Y., Wang, J., He, Y., Xue, G., 2021. The coupling of BOLD signal variability and degree centrality underlies cognitive functions and psychiatric diseases. Neuroimage doi:10.1016/j.neuroimage.2021.118187.
Soldan, A., Pettigrew, C., Zhu, Y., Wang, M.C., Bilgel, M., Hou, X., Lu, H., Miller, M.I., Albert, M., Research Team, BIOCARD, 2021. Association of lifestyle activities with functional brain connectivity and relationship to cognitive decline among older adults. In: Cerebral Cortex, p. bhab187. doi:10.1093/cercor/bhab187 Advance online publication.

Somerville, L.H., Bookheimer, S.Y., Buckner, R.L., Burgess, G.C., Curtiss, S.W., Dapretto, M., Elam, J.S., Gaffrey, M.S., Harms, M.P., Hodge, C., Kandala, S., Kastman, E.K., Nichols, T.E., Schlaggar, B.L., Smith, S.M., Thomas, K.M., Yacoub, E., Van Essen, D.C., Barch, D.M., 2018. The lifespan human connectome project in development: a large-scale study of brain connectivity development in 5-21 year olds. Neuroimage 183, 456–468.

Sporns, O., Betzel, R. F., 2016. Modular Brain Networks. Annual Review of Psychology 67, 613–640.

Sridharan, D., Levitin, D.J., Menon, V., 2008. A critical role for the right fronto-insular cortex in switching between central-executive and default-mode networks. Proc. Natl. Acad. Sci. U.S.A. 105, 12569–12574.

Sumner, J.A., Colich, N.L., Uddin, M., Armstrong, D., McLaughlin, K.A., 2019. Early experiences of threat, but not deprivation, are associated with accelerated biological aging in children and adolescents. Biol. Psychiatry 85, 268–278.

Süss, H., Willi, J., Grub, J., Ehlert, U., 2021. Estradiol and progesterone as resilience markers?–findings from the swiss perimenopause study. Psychoneuroendocrinology 127, 105177.

Sydnor, V.J., Larsen, B., Bassett, D.S., Alexander-Bloch, A., Fair, D.A., Liston, C., Mackey, A.P., Milham, M.P., Pines, A., Roalf, D.R., Seidlitz, J., Xu, T., Raznahan, A., Satterthwaite, T.D., 2021. Neurodevelopment of the association cortices: patterns, mechanisms, and implications for psychopathology. Neuron doi:10.1016/j.neuron.2021.06.016, S0896-6273(21)00457-8. Advance online publication.

Sun, Y., Fang, J., Wan, Y., Su, P., Tao, F., 2020. Association of early-life adversity with measures of accelerated biological aging among children in China. JAMA Network Open 3, e2013588.

Tang, X., Jaenisch, R., Sur, M., 2021. The role of GABAergic signalling in neurodevelopmental disorders. Nat. Rev. Neurosci. 22, 290–307.

Tani, Y., Fujiwara, T., Kondo, K., 2020. Association between adverse childhood experiences and dementia in older japanese adults. JAMA Network Open 3, e1920740.

Thiele, J.A., Faskowitz, J., Sporns, O., Hilger, K., 2022. Multitask brain network reconfiguration is inversely associated with human intelligence. Cerebral Cortex bhab473. doi:10.1093/cercor/bhab473, Advance online publication.

Thompson, A., Schel, M.A., Steinbeis, N., 2021. Changes in BOLD variability are linked to the development of variable response inhibition. Neuroimage 228, 117691.

Tofighi, D., Kelley, K., 2020. Indirect effects in sequential mediation models: evaluating methods for hypothesis testing and confidence interval formation. Multivariate Behav Res 55, 188–210.

Tooley, U.A., Bassett, D.S., Mackey, A.P., 2021. Environmental influences on the pace of brain development. Nat. Rev. Neurosci. 22, 372–384.

Tozzi, L., Staveland, B., Holt-Gosselin, B., Chesnut, M., Chang, S.E., Choi, D., Shiner, M.L., Wu, H., Lerma-Usabiaga, G., Sporns, O., Barch, D., Gotlib, I.H., Hastie, T.J., Kerr, A.B., Poldrack, R.A., Wandell, B.A., Wintermark, M., Williams, L.M., 2020. The human connectome project for disordered emotional states: protocol and rationale for a research domain criteria study of brain connectivity in young adult anxiety and depression. Neuroimage 124, 116715.

Toumbelekis, M., Liddell, B.J., Bryant, R.A., 2021. Secure attachment priming protects against relapse of fear in Young adults. Transl. Psychiatry 11, 584.

Tyborowska, A., Volman, I., Niermann, H., Pouwels, J.L., Smeekens, S., Cillessen, A., Toni, I., Roelofs, K., 2018. Early-life and pubertal stress differentially modulate grey matter development in human adolescents. Sci. Rep. 8, 9201. doi:10.1038/s41598-018-27439-5.

Vandekar, S.N., Shinohara, R.T., Raznahan, A., Roalf, D.R., Ross, M., DeLeo, N., Ruparel, K., Verma, R., Wolf, D.H., Gur, R.C., Gur, R.E., Satterthwaite, T.D., 2015. Topologically dissociable patterns of development of the human cerebral cortex. J. Neurosci. 35, 599–609.

Vink, M., Gladwin, T.E., Geeraerts, S., Pas, P., Bos, D., Hofstee, M., Durston, S., Vollebergh, W., 2020. Towards an integrated account of the development of self-regulation from a neurocognitive perspective: a framework for current and future longitudinal multi-modal investigations. Dev. Cogn. Neurosci. 45, 100829.

Wang, H., Ghaderi, A., Long, X., Reynolds, J.E., Lebel, C., Protzner, A.B., 2021. The longitudinal relationship between BOLD signal variability changes and white matter maturation during early childhood. Neuroimage 242, 118448.

Waschke, L., Kloosterman, N., Obleser, J., Garrett, D.D., 2021. Behaviour needs neural variability. Neuron 109, 1–16.

Watanabe, K., Taskesen, E., van Bochoven, A., Posthuma, D., 2017. Functional mapping and annotation of genetic associations with FUMA. Nat. Commun. 8, 1826.

Winkler, A.M., Renaud, O., Smith, S.M., Nichols, T.E., 2020. Permutation inference for canonical correlation analysis. Neuroimage 220, 117065.

Winter, W., Sheridan, M., 2014. Previous reward decreases errors of commission on later 'No-Go' trials in children 4 to 12 years of age: evidence for a context monitoring account. Dev. Sci. 17, 797–807.

Wojcik, G.L., Graff, M., Nishimura, K.K., Tao, R., Haessler, J., Gignoux, C.R., Highland, H.M., Patel, Y.M., Sorokin, E.P., Avery, C.L., Belbin, G.M., Bien, S.A., Cheng, I., Cullina, S., Hodonsky, C.J., Hu, Y., Huckins, L.M., Jeff, J., Justice, A.E., Kocarnik, J.M., … Carlson, C.S., 2019. Genetic analyses of diverse populations improves discovery for complex traits. Nature 570, 514–518.

Xia, M., Wang, J., He, Y., 2013. Brainnet viewer: a network visualization tool for human brain connectomics. PLoS One 8, e68910.

Yeo, B.T.T., Krienen, F.M., Sepulcre, J., Sabuncu, M.R., Lashkari, D., Hollinshead, M., … Buckner, R.L., 2011. The organization of the human cerebral cortex estimated by intrinsic functional connectivity. J. Neurophysiol. 106, 1125–1165.

Zacharopoulos, G., Sella, F., Cohen Kadosh, R., 2021. The impact of a lack of mathematical education on brain development and future attainment. Proc. Natl. Acad. Sci. U.S.A. 118, e2013155118.